



## Identification of dominant phytoplankton functional types in the Mediterranean Sea based on a regionalized remote sensing approach

G. Navarro <sup>a,\*</sup>, S. Alvain <sup>b,c</sup>, V. Vantrepotte <sup>b,c</sup>, I.E. Huertas <sup>a</sup>

<sup>a</sup> Departamento de Ecología y Gestión Costera, Instituto de Ciencias Marinas de Andalucía (ICMAN-CSIC), 11510 Puerto Real, Cádiz, Spain

<sup>b</sup> Université de Lille Nord de France, F-59000 Lille, France

<sup>c</sup> Laboratoire d'Océanologie et Géosciences, LOG, UMR 8187, CNRS, ULCO, F-62930 Wimereux, France



### ARTICLE INFO

#### Article history:

Received 19 November 2013

Received in revised form 23 May 2014

Accepted 23 June 2014

Available online xxxx

#### Keywords:

Ocean color

Phytoplankton functional types

PHYSAT

Mediterranean Sea

### ABSTRACT

During the last decade, the analysis of the ocean color satellite imagery has allowed determining the dominant phytoplankton groups in surface waters through the development of bio-optical models aimed at identifying the main phytoplankton functional types (PFTs) or size classes from space. One of these bio-optical model is PHYSAT, which is a global method applied for oceanic Case I water and used to identify in satellite pixels specific dominant phytoplankton groups, such as nanoeukaryotes, *Prochlorococcus*, *Synechococcus*, diatoms, *Phaeocystis*-like and coccolithophores. Here, we present a regionalized version of the PHYSAT method that has been specifically developed for the Mediterranean Sea due to the peculiarities of phytoplankton assemblages and succession than can be found in the basin and its particular optical properties. The updated version of the method, the so called PHYSAT-Med, has been validated successfully with large in situ datasets available for this oceanic region, mainly for nanoeukaryotes, *Prochlorococcus*, *Synechococcus* and diatoms. PHYSAT-Med allows to include a much higher number of pixels for the Mediterranean than PHYSAT does, through the use of a new Look-Up-Table created specifically for this oceanic region. Results provided by PHYSAT-Med showed the dominance of *Synechococcus* versus prochlorophytes throughout the year at the basin level, although nanoeukaryotes were more abundant during winter months. In addition, PHYSAT-Med data identified a rise in the eukaryote biomass (mainly diatoms) during the spring period (March to April), especially in the Ligurian and Adriatic seas. PHYSAT-Med represents a useful tool for the spatio-temporal monitoring of different dominant phytoplankton functional types in Mediterranean surface waters at a high resolution.

© 2014 Elsevier Inc. All rights reserved.

### 1. Introduction

The Mediterranean Sea is the largest semi-enclosed sea on Earth and is considered one of the most complex marine environments where much remains to be known with regard to circulation dynamics, biogeochemistry and biological activity (Tanhua et al., 2013). The Mediterranean Sea presents a deficit hydrological balance, as evaporation exceeds the supply of fresh water from streams and precipitation. This deficit is partially compensated by the inflow of Atlantic waters through the Strait of Gibraltar, which penetrates into the basin as a surface current that is less salty and less dense than the deeper counter current of the Mediterranean outflow. This export of intermediate depth water to the Atlantic directly influences the oceanographic conditions in the North Atlantic (Peliz et al., 2009) and its biogeochemical inventories (Flecha et al., 2012; Huertas et al., 2012). The Mediterranean is sensitive to climatic changes and hence monitoring the evolution of

its dynamics and biogeochemistry is essential not only for the basin itself but also for the Atlantic Ocean.

Hydrological differences along the basin cause the presence of an increasing oligotrophy gradient from west to east in the Mediterranean, which can be evidenced by both satellite data and in situ measurements. A decreasing chlorophyll-a (Chla) gradient from north to south has been also described, with the exception of a high Chla region detected along the Algerian coast (see review by Siokou-Frangou et al., 2010). Overall, low chlorophyll concentrations are present over large areas in the Mediterranean although local phytoplankton blooms that can be regularly found in the Liguro-Provencal region, Alborán Sea and the Catalan–North Balearic front (Ignatiades, Gotsis-Skretas, Pagou, & Krasakopoulou, 2009). The nutrients and chlorophyll-a pools rank the basin as oligotrophic to ultraoligotrophic (Antoine, Morel, & Andre, 1995; Krom, Kress, Brenner, & Gordon, 1991).

In oligotrophic waters, phytoplankton community is mainly composed by picoplankton and ultraplankton (Brunet, Casotti, Vantrepotte, Corato, & Conversano, 2006; Dandonneau, Montel, Blanchot, Giraudeau, & Neveux, 2006; Li et al., 1983; The MerMex Group, 2011). In the Mediterranean, on the other hand, phytoplankton community reveals a considerable diversity variability over spatial and temporal scales

\* Corresponding author at: Instituto de Ciencias Marinas de Andalucía (ICMAN-CSIC), Campus Universitario Río San Pedro, Avda. República Saharaui, nº2, 11519 Puerto Real, Cádiz, Spain. Tel.: +34 956 83 26 12; fax: +34 956 83 47 01.

E-mail address: [gabriel.navarro@icman.csic.es](mailto:gabriel.navarro@icman.csic.es) (G. Navarro).

(Siokou-Frangou et al., 2010) and large dissimilarities in phytoplankton species composition and other microorganisms across the basins have been highlighted. The picture emerging from many studies shows the dominance of the picoplankton as the fingerprint of the Mediterranean Sea and its overriding oligotrophy but local physical structures that allow the formation of phytoplankton blooms cause the coexistence of more microalgal groups (Siokou-Frangou et al., 2010). An extensive amount of information on the phytoplankton community structure along the Mediterranean coastline is available. On the contrary, longitudinal data based on large-scale investigations in open ocean waters are scarce in the literature (Ignatiades et al., 2009).

This lack of measurements can be partly overcome by using new tools, such as remote sensing techniques. During the last decade and based on different approaches, several algorithms are now able to detect phytoplankton functional types (PFTs) or size classes from space (Aiken et al., 2009; Alvain, Moulin, & Dandonneau, 2008; Alvain, Moulin, Dandonneau, & Breon, 2005; Brewin et al., 2010; Ciotti & Bricaud, 2006; Hirata et al., 2009; Raitsos et al., 2008; Sathyendranath et al., 2004; Uitz, Claustre, Morel, & Hooker, 2006). Platt, Sathyendranath, and Stuart (2006) concluded that the detection of different phytoplankton groups from remote sensing images was a major challenge in ocean optics.

The PFTs are groups of species that play specific roles in the marine biogeochemical cycles and trophic flows (see Le Quéré et al., 2005; Nair et al., 2008; Rudorff & Kampel, 2011). One of the methods that enables to detect PFTs from space is the so called PHYSAT (Alvain et al., 2005, 2008), which was specifically developed to identify the dominant phytoplankton groups from ocean color measurements. Briefly, PHYSAT is a global model applied for oceanic Case I water and is designed to detect satellite pixels in which the dominant groups are nanoeukaryotes (and separately *Phaeocystis*-like and coccolithophores), two types of picoplankton (*Prochlorococcus* and *Synechococcus*-like cyanobacteria) and diatoms (Alvain et al., 2008). PHYSAT is based on the analysis of normalized water-leaving radiance (nLw, Table 1) measurements anomalies, computed after removal the impact chlorophyll *a* variations. Specific nLw spectra anomalies (in terms of shapes and amplitudes) have been empirically associated to the presence of dominant phytoplankton groups, based on in situ biomarkers pigments observations. (Alvain et al., 2005, 2008, 2012; Ben Mustapha, Alvain, Jamet, Loisel, & Dessailly, 2014). Alternative methods have been also applied to detect distinct phytoplankton groups, for instance, diatoms (Sathyendranath et al., 2004), the cyanobacteria *Synechococcus* (Morel, 1997), the N<sub>2</sub>-fixing cyanobacteria *Trichodesmium* (Subramaniam, Brown, Hood, Carpenter, & Capone, 1999, 2001; Subramaniam, Carpenter, & Falkowski, 1999), *Phaeocystis globosa* (Astoreca et al., 2009; Lubac et al., 2008) and coccolithophores (Ackleson, Balch, & Holligan, 1994;

Brown & Podestá, 1997; Brown & Yoder, 1994; Cokacar, Kubilay, & Oguz, 2001; Gordon et al., 2001; Iglesias-Rodríguez et al., 2002; Kopelevich et al., 2013; Moore, Dowell, & Franz, 2012; Smyth, Moore, Groom, Land, & Tyrell, 2002; Tyrell, Holligan, & Mobley, 1999). Nevertheless, the PHYSAT method allows to distinguish several groups of phytoplankton simultaneously and identifies the dominant PFT at each particular pixel and at each point in time. This method has been successfully validated and used in recent years (Alvain et al., 2005, 2006, 2008, 2012, 2013; Arnold et al., 2010; Belviso et al., 2012; Ben Mustapha et al., 2014; Bopp, Aumont, Cadule, Alvain, & Gehlen, 2005; D'Ovidio, De Monte, Alvain, Dandonneau, & Levy, 2010; De Monte, Soccodato, Alvain, & d'Ovidio, 2013; Demarcq, Reygondeau, Alvain, & Vantrepotte, 2012; Gorgues et al., 2010; Hashioka et al., 2013; Masotti et al., 2010, 2011). Results were satisfactory for nanoeukaryotes (82%) and a decrease in the percentage of successful retrieval was observed for diatoms (73%), *Synechococcus* (57%) and *Prochlorococcus* (61%) (Alvain et al., 2012).

However, due to the specific character of phytoplankton assemblages in the Mediterranean Sea and their associated bio-optical relationships that can be affected by continental inputs such as rivers discharge and desert dust events (Alvain et al., 2006; Bricaud, Bosc, & Antoine, 2002; Claustre et al., 2002; Loisel et al., 2011), it is necessary to adapt the PHYSAT method and evaluate its derived results in this specific ocean region. In fact, Santoleri, Volpe, Marullo, and Nardelli (2008) pointed out that the difference in bio-optical characteristics at the regional scale in Mediterranean Sea is due to ecological reason such as the presence of specific phytoplankton groups. Moreover, the presence of the aerosols due to anthropogenic atmospheric emissions from continental Europe and Saharan dust makes it difficult to apply standard remote sensing procedures for the atmospheric correction (Moulin et al., 1997). In fact, the presence and abundance of aerosols is one of the factors determining the different optical properties of the Mediterranean with respect to the global ocean (Claustre et al., 2002). Therefore, during the last years, many regional algorithms have been developed for the Mediterranean Sea, such as DORMA-SeaWiFS (D'Ortenzio, Marullo, Ragni, d'Alcala, & Santoleri, 2002), BRIC-SeaWiFS (Bricaud et al., 2002), MedOC4-SeaWiFS (Volpe et al., 2007), MedOC3-MODIS (Santoleri et al., 2008) and MedOC4ME-MERIS (Santoleri et al., 2008) since standard algorithms overestimate low Chla and conversely, underestimate high concentrations.

In this work, the previous version of PHYSAT (Alvain et al., 2005, 2008) has been modified in order to estimate the most frequent phytoplankton groups in the Mediterranean Sea. The updated version (hereafter PHYSAT-Med) has been validated using in situ measurements collected in different cruises conducted throughout the entire basin. Therefore, the main objectives of this study were: (i) to adapt

**Table 1**  
Acronyms information.

Acronym	Name	Units	Explanation
Chl <i>a</i>	Chlorophyll <i>a</i> concentration	mg m <sup>-3</sup>	Chlorophyll <i>a</i> concentration
OC3M-Chla	Chlorophyll <i>a</i> concentration	mg m <sup>-3</sup>	Chla estimated by standard OC3M algorithm for MODIS images
MedOC3-Chla	Chlorophyll <i>a</i> concentration	mg m <sup>-3</sup>	Chla concentration estimated by regional MedOC3 algorithm for MODIS images
K490	Diffuse attenuation coefficient at 490 nm	m <sup>-1</sup>	The diffuse attenuation coefficient in water indicates how strongly light intensity at a specified wavelength is attenuated within the water column.
nLw	Normalized water-leaving radiance	mW cm <sup>-2</sup> μm <sup>-1</sup>	The upwelling radiance just above the sea surface, in the absence of an atmosphere, and with the sun directly overhead
nLw <sup>ref</sup>	Specific water-leaving radiance	mW cm <sup>-2</sup> μm <sup>-1</sup>	Represents the average nLw spectrum for a given value of Chla. This reference is used to remove the first order effect of Chla on nLw(λ) measurements.
LUT	Look-Up-Table		Look-Up-Table of nLw <sup>ref</sup> for a given λ and Chla concentration
Rrs	Remote sensing reflectance	Adimensional	Upwelling radiance emerging from the ocean divided by the downwelling irradiance reaching the water surface
F <sub>0</sub>	Mean solar irradiance	mW cm <sup>-2</sup> μm <sup>-1</sup>	Mean solar irradiance to convert nLw into Rrs
Ra	Radiance anomalies	Adimensional	Represents the second order variation of the nLw after removal the first order effect of the Chla variation. Ra is independent of the Chla levels and represents the second order variation of nLw(λ)

the original PHYSAT method to the Mediterranean Sea for MODIS satellite images datasets; (ii) to validate the new PHYSAT-Med method with in situ measurements and (iii) to evaluate the spatio-temporal patterns of the PFTs in the Mediterranean Sea for MODIS era.

## 2. Material and methods

### 2.1. PHYSAT method

The PHYSAT method is based on the identification of specific signatures in the normalized water leaving radiance ( $nLw$ , Table 1) spectra measured by an ocean color sensor (Alvain et al., 2005, 2008). This approach considers the analysis of the second order variation in  $nLw$  measurements after removal of the impact of chlorophyll *a* variation. The first version (PHYSAT-v2005; Alvain et al., 2005) established the relationship between SeaWiFS- $nLw$  measurements anomalies and four phytoplankton groups, such as diatoms, nanoeukaryotes, *Synechococcus* and *Prochlorococcus* for a wide range of water types (Alvain et al., 2005) such as the North Atlantic and the Equatorial and South Pacific. The second version of PHYSAT (PHYSAT-v2008, Alvain et al., 2008) included additional phytoplankton groups as “Phaeocystis-like” and cocolithophorids. The latest version used the new specific water leaving radiance ( $nLw^{ref}$ , see Table 1) model that considered all the SeaWiFS data available for all the geographical areas during the same year, including diatoms data from Southern Ocean that had been excluded in the former versions (PHYSAT-v2005). This modification led to slight changes in the criteria used to identify the four initial phytoplankton groups. Alvain et al. (2008) presented a new Look-Up-Table (LUT) with the characteristics of specific radiance anomalies ( $Ra$ , see Table 1) spectra for six phytoplankton groups that could be detected with the PHYSAT-v2008 method. Although PHYSAT is empirically based on radiance anomalies, recently Alvain et al. (2012) have provided a theoretical explanation to understand the derived results, showing that each phytoplankton group is generally associated with a specific bio-optical environment, represented by different values of particulate scattering ( $b_p$ ), absorption by the colored dissolved organic matter ( $a_{cdom}$ ) and the absorption by the phytoplankton ( $a_{phy}$ ). In addition, PHYSAT has been successfully applied to other ocean color sensors, such as Coastal Zone Color Scanner – CZCS (Masotti, Alvain, Moulin, & Antoine, 2009) and Ocean Colour and Temperature Sensor – OCTS (Masotti et al., 2009, 2011). In this work, we have incorporated the PHYSAT-v2008 version and adapted to the Mediterranean Sea using the MODIS dataset. Fig. 1 displays a schematic diagram of the steps followed to adapt PHYSAT-Med.

#### 2.1.1. Step 1: satellite data

All Level 3 MODIS daily products (reprocessing version R2013.0) at 4-km resolution acquired from NASA Oceanscolor website (<http://oceancolor.gsfc.nasa.gov>) during more than a decade (since July 2002 to May 2013) were downloaded (Fig. 1, step 1) and remapped on an equi-rectangular grid on the Mediterranean area ( $-6$  to  $36^\circ$  E and  $30$  to  $46^\circ$  N, Fig. 2). The Black Sea was masked, as its dynamics follow an independent regime and was considered distinct from the rest of the basin (Oguz, Tugrul, Kideys, Ediger, & Kubilay, 2004). These products were chlorophyll-*a* concentration ( $Chla$ ), estimated by the global standard algorithm OC3M- $Chla$  (O'Reilly et al., 1998, 2000), aerosol optical thickness at 869 nm (AOT), diffuse attenuation coefficient at 490 nm ( $K_{490}$ ) and remote sensing reflectance ( $Rrs(\lambda)$ ) at 412, 443, 469, 488, 531, 547 and 555 nm.

Since the global chlorophyll algorithm generally leads to a significant overestimation in the Mediterranean Sea (Bricaud et al., 2002; Claustré et al., 2002; D'Ortenzio & d'Alcalá, 2009; Volpe et al., 2007), the regional MedOC3- $Chla$  algorithm for MODIS images (Santoleri et al., 2008) was considered to estimate the chlorophyll *a* concentration in the Mediterranean Sea. This MedOC3- $Chla$  algorithm is an adaptation of the Mediterranean bio-optical algorithm (MedOC4) developed initially by

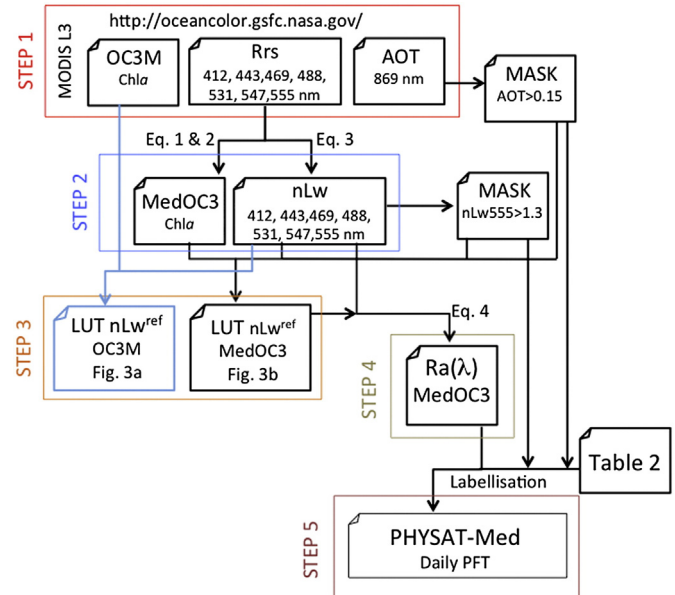


**Fig. 1.** Schematic view of steps followed to adapt PHYSAT-Med.

Volpe et al. (2007) for SeaWiFS images. Therefore, daily images of chlorophyll *a* concentration using MedOC3- $Chla$  algorithm (Fig. 1, step 2):

$$MedOC3-Chla = 10^{(0.380 - 3.688R + 1.036R^2 + 1.616R^3 - 1.328R^4)} \quad (1)$$

where

$$R = \log_{10} \left( \frac{Rrs443 - Rrs488}{Rrs555} \right). \quad (2)$$

This bio-optical algorithm is based, like OC3M, on fourth-power polynomial regression between log-transformed  $Chla$  and log-transformed maximum band ratio (MBR). It is known that using multiple  $Rrs$  ratios decreases the noise-to-signal ratio and thereby enhancing the algorithm's performance (O'Reilly et al., 1998). MedOC3 algorithm was calibrated on a representative open-water bio-optical dataset collected in the Mediterranean Sea, and is declared to match the requirements of unbiased satellite chlorophyll *a* estimation (Santoleri et al., 2008).

At the second step, the remote sensing reflectance ( $Rrs$ ) was converted to  $nLw$  using the nominal band solar irradiance ( $F_o$ , in  $mW\ cm^{-2}\ \mu m^{-1}$ ) for any specific spectral band ( $\lambda$ ) for MODIS sensor (Fig. 1).

$$nLw_{(\lambda)} = Rrs_{(\lambda)} * F_{o(\lambda)}. \quad (3)$$

Following PHYSAT methodology (Alvain et al., 2005, 2008), a two new Look-Up-Table (Fig. 1, step 3) of  $nLw^{ref}(\lambda, Chl-a)$  was empirically generated for the Mediterranean Sea from a large dataset of MODIS  $Chla$  and  $nLw$  pixels for all daily images comprised within the study period (July 2002 to May 2013). Turbid pixels (defined as  $nLw_{555} > 1.3\ mW\ cm^{-2}\ mm^{-1}\ sr^{-1}$ , Nezlin & DiGiacomo, 2005) and pixels with AOT higher than 0.15 (Alvain et al., 2005) were excluded in order to minimize the impact of high suspended matter loads as well as atmospheric correction error and clouds boundaries respectively. Briefly,  $nLw^{ref}$  is calculated from  $nLw$  data and the associated  $Chla$  computed from the OC3M- $Chla$  (Fig. 3a) and MedOC3 (Fig. 3b) algorithms within the chlorophyll *a* range between 0.01 and  $10\ mg\ m^{-3}$  (41 narrow intervals). Note that this latter threshold is higher than that of the original PHYSAT method ( $3\ mg\ m^{-3}$ ; Alvain et al., 2005) in order to maximize the incorporation of all values obtained by the in

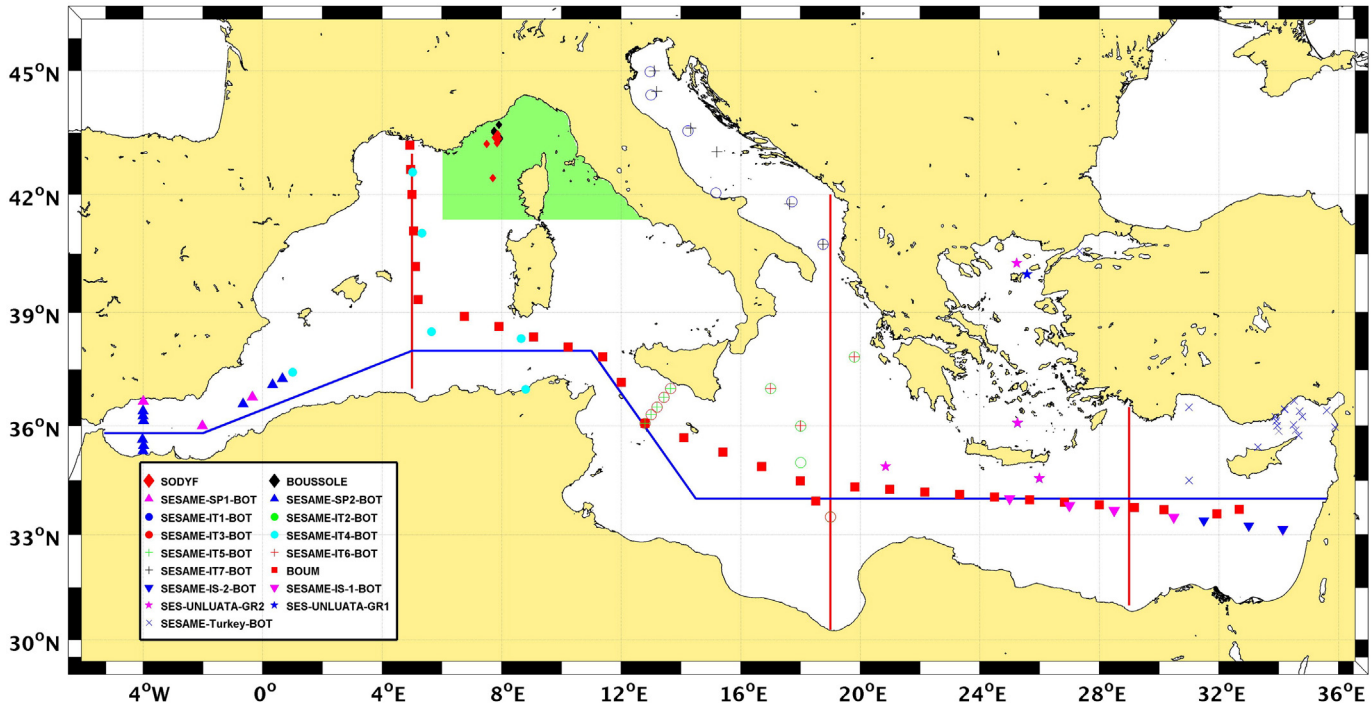


**Fig. 2.** Map of in situ sampling stations (see Table 3). Blue and red lines indicate the position of the four transects used to extract PFT data. Green area shows the Ligurian Sea region (Bricaud et al., 2002). (For interpretation of the references to color in this figure legend, the reader is referred to the web version of this article.)

situ measurements, as maximum chlorophyll *a* estimations around 8 mg m<sup>-3</sup> can be found in the Alboran Sea (Arin, Morán, & Estrada, 2002). In addition, a Look-Up-Table at global scale for MODIS sensor is also displayed in Fig. 3c (data obtained from PHYSAT website, <http://log.univ-littoral.fr/Physat>).

Once the new LUT for the Mediterranean Sea was calculated using regional MedOC3-Chla algorithm (Fig. 3b), the radiance anomalies ( $Ra(\lambda)$ , Fig. 1, step 4) were computed for all daily MODIS wavelengths analyzed using the following equation (Eq. 4) for all wavelengths available (412, 443, 469, 488, 531, 547 and 555 nm), where  $Ra(\lambda)$  is an adimensional unit parameter and by definition, this parameter is independent of the chlorophyll *a* level (being by extension independent of the biomass) and represents hence the second order variation of  $nLw(\lambda)$ .

$$Ra(\lambda) = \frac{nLw_{(\lambda)}}{nLw_{ref}}. \quad (4)$$

The radiance anomaly represents the second order variation of the normalized water-leaving radiances after removal the first order effect of the Chla variation (Alvain et al., 2005).

The new LUT (Fig. 3b) can be assumed to include both the mean ocean color signal and potential differences between the MODIS sensor and the previously used SeaWiFS sensor, allowing to use with confidence classical thresholds on anomalies (see Table 5 in Alvain et al., 2005 and Table 1 in Alvain et al., 2008). The shape and amplitude of the Ra spectra mainly depend on the bio-optical environment, represented by different values of the  $b_p$ ,  $a_{cdom}$  and  $a_{phy}$ , as it has been proven by the sensitivity study of Ra made by Alvain et al. (2012). These analyses showed that for a given chlorophyll concentration, the particle scattering variability explains the largest part of the remotely sensed Ra spectral variability, especially when focusing on Ra magnitude changes. However, variations in colored dissolved organic matter and phytoplankton absorption coefficients can also have a large impact on Ra with specific spectral signatures.

### 2.1.2. Spectral characterization of phytoplankton groups

As noted above, Alvain et al. (2005) established the thresholds of Ra for each of the four phytoplankton groups analyzed in PHYSAT-v2005 (see Table 5 in Alvain et al., 2005). This table was subsequently updated with two more phytoplankton groups and some thresholds were hence modified (see Table 1 in Alvain et al., 2008). Recently, Ben Mustapha et al. (2014) have provided the spectral signatures of Ra corresponding to the four PHYSAT-SOM labeled classes. In our study, we have established new characteristics of acceptable Ra spectra (Table 2) for MODIS wavelengths using the linear interpolation between SeaWiFS and MODIS wavelengths and the Ra thresholds described by Alvain et al. (2008). This can be done considering the relatively flat signals used in PHYSAT and the very close wavelengths of the two sensors.

The new thresholds described in Table 2 were used to process daily images to calculate daily PFTs maps (Fig. 1, step 5). For a spectra to be associated with one group, all criteria must be fulfilled. These thresholds (Table 2) have been fixed in order to avoid any overlapping. This labeling step consists in relating the Ra spectral patterns to in situ pigment inventories assigning each to a particular phytoplankton group (labelling procedure). Pixels with nLw values that were not classified for any phytoplankton groups summarized in Table 2, based on available in situ information for the calibration step of PHYSAT, were catalogued as “unidentified (unid.”). These unidentified pixels are due to the fact that Ra spectra of these pixels have not been labeled although it is worthy to note that the number of unidentified pixels could diminish when more additional in situ information is available. These situations could lead to no-classification or misclassification of the radiometric signal in terms of phytoplankton groups. However, most of these cases lead to no-classification or unidentification rather than to a misclassification. The remaining misclassification cases lead to wrong identification and explain the wrong identifications found during the previous PHYSAT validation exercise (Alvain et al., 2012).

From this image database (near to 4000 daily images), 10-days and monthly maps of dominant phytoplankton group detection were obtained by calculating at each geographical pixel, the phytoplankton group present during more days during the integration period (10-days or

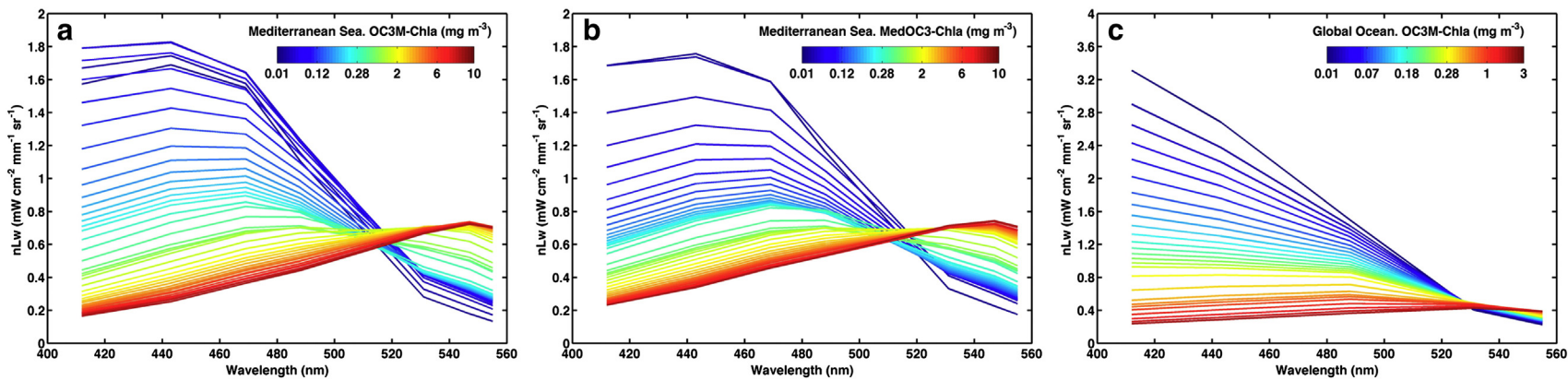


**Fig. 3.** MODIS reference model ( $nLw^{\text{ref}}(\lambda, \text{Chla})$ ) of the normalized water-leaving radiance ( $nLw$ ) as a function of wavelength for various Chla concentrations (color scale, in  $\text{mg m}^{-3}$ ) for the Mediterranean Sea (excluding Black Sea) during the study period (July 2002–May 2013) using a) standard algorithm for chlorophyll-*a* (OC3M-Chla), b) regional algorithm (MedOC3-Chla). c)  $nLw^{\text{ref}}(\lambda)$  at global scale for MODIS sensor (data obtained from PHYSAT website, <http://log.univ-littoral.fr/Physat>).

**Table 2**

Characteristics of acceptable Ra spectra for each phytoplankton groups.

MODIS wavelengths (nm)	412	443	469	488	531	547	555	Additional criteria
Phytoplankton groups								
Nanoeucaryotes min.	0.4	0.55	0.5777	0.5979	0.6	0.6	0.6	$nLw^*412 < nLw^*443$
Nanoeucaryotes max.	0.8	0.9	0.9277	0.9479	1	1	1	$nLw^*443 < nLw^*488$
<i>Prochlorococcus</i> min.	0.8	0.9	0.9	0.9	0.9	0.9	0.9	
<i>Prochlorococcus</i> max.	1	1	1	1	1	1	1	
<i>Synechococcus</i> min.	1	1	1	1	1	1	1	
<i>Synechococcus</i> max.	1.2	1.2	1.1723	1.1521	1.15	1.15	1.15	$nLw^*412 > nLw^*488$
Diatoms min.	1.2	1.2	1.1723	1.1521	1.15	1.15	1.15	$nLw^*555 < nLw^*488$
Diatoms max.	2.2	1.8	1.6340	1.5128	1.4	1.4	1.4	$nLw^*412 < nLw^*443$
<i>Phaeocystis</i> min.	1.3	1.4	1.4	1.4	1.4	1.4	1.4	$nLw^*443 < nLw^*488$
<i>Phaeocystis</i> max.	1.5	1.6	1.6	1.6	1.6	1.6	1.6	$nLw^*531 > nLw^*555$
Coccolithophorids min.	2.5	2.5	2.5	2.5	2.5	2.5	2.5	
Coccolithophorids max.	6	6	6	6	6	6	6	

monthly respectively), including the “unidentified” pixels. Map of detection frequencies over each month, between 0 (group never detected) and 1 (all valid pixels were associated with the group), were also calculated to each group from the entire dataset.

## 2.2. In situ validation

High-performance liquid chromatography (HPLC) allows the quantification of a suite of accessory pigments (carotenoids and chlorophylls) in phytoplankton. Accordingly, the chemotaxonomic correspondence of HPLC-determined pigments can be used to study the phytoplankton community composition (e.g. Claustre & Marty, 1995; Gieskes, Kraay, Nontji, Setiapermana, & Sutomo, 1988; Goericke & Repeta, 1993; Mackey, Mackey, Higgins, & Wright, 1996) as these pigments are specific of individual phytoplanktonic taxa or groups (Jeffrey & Veske, 1997; Mackey et al., 1996; Uitz et al., 2006; Vidussi, Claustre, Manca, Luchetta, & Marty, 2001). However, some pigments may covary with others or be redundant, which makes data interpretation and visualization tedious.

In this study, more than 3000 HPLC measurements collected in the Mediterranean Sea have been analyzed (Table 3). The data source is composed by data from DYFAMED Time Series obtained from MAREDAT global database of HPLC (Peloquin et al., 2013), the BOUSSOLE project

(i.e. Antoine et al., 2006; Organelli, Bricaud, Antoine, & Uitz, 2013) and the SESAME Project database (Ras, Claustre, Xing, & Uitz, 2011). Fig. 2 displays the spatial location of the in situ HPLC measurements used in this study that covers a wide range of water types in the Mediterranean Sea. All these HPLC analysis were carried out by the members of the SAPIGH analytical platform from the *Laboratoire d'Océanographie de Villefranche (LOV)*, following the protocol described in Marty, Chiavérini, Pizay, and Avril (2002) for DYFAMED Time Series, Vidussi et al. (2001) and Antoine et al. (2006) for BOUSSOLE project and Ras, Uitz, and Claustre (2008) for SESAME cruises.

Here, we only considered samples limited to the first optical depth, which reduces the number of available pigment inventories to 1382 samples. The first optical depth is the depth at which 90% of the light originates for remote sensing purposes (Trees, Clark, Bidigare, Ondrusk, & Mueller, 2000) and was calculated from  $K_{490}$  daily MODIS images according to the following equation:

$$\text{Optical depth} = 1/K_{490} \quad (5)$$

where daily  $K_{490}$  images were downloaded from the oceancolor website. When daily  $K_{490}$  value for the matchup HPLC in situ data was missing, a climatology values for optical depth were included.

**Table 3**

Cruises, location, sampling period and season, dataset and number of HPLC samples (in brackets number in first optical depth).

Cruises	Location	Period	Season	Dataset	n
SODYFT	Ligurian Sea	02/25/2002–12/19/2005	All	DYFAMED <sup>1</sup>	451 (160)
BOUSSOLE	Ligurian Sea	07/22/2001–11/10/2007	All	BOUSSOLE <sup>2</sup>	1877 (1113)
SESAME_IT1_BOT	Adriatic Sea	02/16/2008–02/25/2008	Spring	SESAME <sup>3</sup>	34 (21)
SESAME_IT2_BOT	Ionian Sea	03/02/2008–03/08/2008	Spring	SESAME <sup>3</sup>	47 (16)
SESAME_IT3_BOT	Ionian Sea	03/17/2008–03/18/2008	Spring	SESAME <sup>3</sup>	44 (16)
SESAME_IT4_BOT	Western Basin	03/20/2008–04/05/2008	Spring	SESAME <sup>3</sup>	58 (24)
SESAME_IT5_BOT	Ionian Sea	09/16/2008–09/26/2008	Autumn	SESAME <sup>3</sup>	45 (20)
SESAME_IT6_BOT	Ionian Sea	09/20/2008–09/23/2008	Autumn	SESAME <sup>3</sup>	28 (11)
SESAME_IT7_BOT	Adriatic Sea	10/09/2008–10/13/2008	Autumn	SESAME <sup>3</sup>	34 (21)
SESAME_SP1_BOT	Alborán Sea	04/08/2008–04/11/2008	Spring	SESAME <sup>3</sup>	15 (5)
SESAME_SP2_BOT	Alborán Sea	09/20/2008–09/27/2008	Autumn	SESAME <sup>3</sup>	62 (39)
SESAME_Turkey_BOT	Levantine Basin	03/20/2008–04/26/2008	Spring	SESAME <sup>3</sup>	78 (34)
SESAME_Turkey_BOT	Levantine Basin	09/19/2008–10/19/2008	Autumn	SESAME <sup>3</sup>	22 (10)
SESAME-IS-1_BOT	Levantine Basin	04/08/2008–04/09/2008	Spring	SESAME <sup>3</sup>	20 (6)
SESAME-IS-2_BOT	Levantine Basin	09/07/2008–09/12/2008	Autumn	SESAME <sup>3</sup>	55 (14)
SES_UNLUATA_gr1	Levantine Basin	03/27/2008–04/06/2008	Spring	SESAME <sup>3</sup>	26 (12)
SES_UNLUATA_gr2	Aegean Sea	08/29/2008–09/07/2008	Autumn	SESAME <sup>3</sup>	32 (12)
BOUM_bot	Mediterranean Sea	06/21/2008–07/18/2008	Summer	SESAME <sup>3</sup>	299 (64)

Data sources:

<sup>1</sup> <http://doi.pangaea.de/10.1594/PANGAEA.793246>.<sup>2</sup> <http://www.obs-vlfr.fr/Boussole/html/home/home.php>.<sup>3</sup> [http://isramar.ocean.org.il/perseus\\_data/CastMap.aspx](http://isramar.ocean.org.il/perseus_data/CastMap.aspx).

### 2.2.1. Identification of phytoplankton groups in HPLC measurements

Many pigments are specific of individual phytoplanktonic taxa or groups (Jeffrey & Vesk, 1997). A review of taxonomic pigments can be found in Jeffrey (1997). They can thus be used as biomarkers of phytoplankton groups (e.g., Gieskes et al., 1988), and with some cautions, assigned to different size classes, such as microphytoplankton, nanophytoplankton and picophytoplankton (Vidussi et al., 2001). For instance, divinyl chlorophyll-a is the typical marker of prochlorophytes (Claustre & Marty, 1995; Goericke & Repeta, 1992; Vidussi et al., 2001), whereas Chla is the universal descriptor of the rest of phytoplankton taxa. Fucoxanthin is the principal marker of diatoms (Jeffrey, 1980) even though it is also present in prymnesiophytes and chrysophytes (Jeffrey & Vesk, 1997). 19'-hexanoyloxyfucoxanthin (19'HF) concentration was mainly related to prymnesiophytes (Latasa, Estrada, & Delgado, 1992; Wright & Jeffrey, 1987) and peridinin, which appears only in traces, is present in small dinoflagellates that can be heterotrophic (Jeffrey & Hallegraeff, 1987). This pigment has not been found in significant amounts in oceanic natural samples of mixed populations containing dinoflagellates, although part of them should have been presumably autotrophic (Latasa et al., 1992). Alloxanthin is another pigment typical of the cryptomonads and is also present in the ciliate *Mesodinium rubrum* (Gieskes & Kraay, 1983; Latasa et al., 1992), but the occurrence of these organisms in NW Mediterranean Sea were too low and erratic to be used in a ratio (Latasa et al., 1992). Finally, zeaxanthin is associated with cyanobacteria (Guillard, Murphy, Foss, & Liaen-Jensen, 1985) although it is also present in prochlorophytes (Chisholm, 1992; Goericke & Repeta, 1992) and also a marker of protection in green algae (Brunet et al., 2006).

As indicated above, we have used the method described by Alvain et al. (2005) to associate dominant phytoplankton groups with in situ HPLC pigment inventory. Pigments ratios ( $P_{\text{rel}}$ ) were defined as:

$$P_{\text{rel}} = \frac{P}{(\text{Chla} + d\text{-Chla})} \quad (5)$$

where P is the measured pigment concentration in the seawater, Chla and d-Chla are the concentrations of chlorophyll-a and divinyl Chla respectively. Alvain et al. (2005, see Table 4) established a threshold of relative pigments concentration to a specific phytoplankton group based on an extended analysis of previous literature. This approach based on biomarker pigment ratio thresholds was used recently at global scale (PHYSAT-SOM, Ben Mustapha et al., 2014). The added-value of the PHYSAT approach is that any phytoplankton group could be added to the method as more in situ observation of dominant phytoplankton groups and pigments data are made available allowing comparing the Ra spectra for these waters and include these new spectral characteristics in Table 2.

## 3. Results

In this study, phytoplankton in situ measurements available for the entire Mediterranean Sea (Fig. 2) from different sources and databases (see Table 3) have been considered, thereby including oligotrophic areas in the middle and eastern part of the basin and local eutrophic regions originated either by upwelling processes in the Alboran Sea or by the winter convergence in the Ligurian Sea. Fig. 4 shows the monthly climatology of the most frequent phytoplankton groups estimated by PHYSAT-Med method in Mediterranean Sea during the study period in the first optical depth. The monthly climatological distributions show that *Synechococcus* is the most dominant phytoplankton group at a basin level during spring-summer months, whereas nanoeukaryotes are more abundant during autumn-winter seasons. In coastal areas proliferate other groups, as it is the case of diatoms with a dominant presence in the northern Adriatic Sea, Ligurian Sea and Gulf of Lion, overall during the spring season. The analysis of the monthly distribution of phytoplankton groups reveals a high spatial and temporal variability

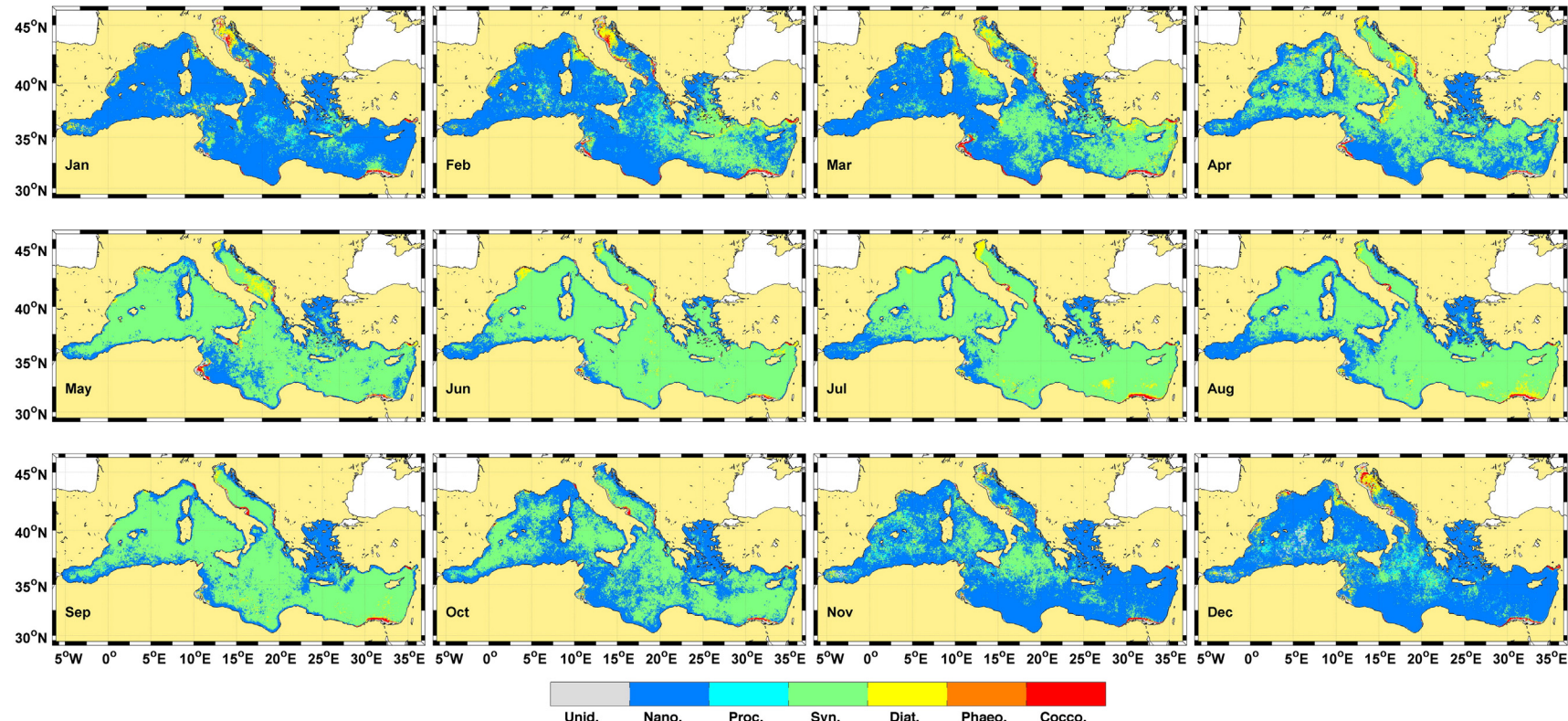
(see Supplementary material). It is evident that *Synechococcus* and nanoeukaryotes are the most abundant PFT in the basin over the year, although other phytoplankters can be identified in different sub-basins. For instance, during the spring season, diatom blooms are clearly distinguishable in several areas of the Mediterranean, such as the Catalan Sea, the Adriatic Sea, the Ligurian Sea and the Ionian Sea. Moreover, coccolithophorids occur over the coastline associated to the vicinity of the large river mouths, such as the Nile, Ebro, and Rhone.

Fig. 5 shows the map of detection frequencies (mean and standard deviation) for four PTF groups considering the unidentified pixels: nanoeukaryotes, *Prochlorococcus*, *Synechococcus* and diatoms. *Synechococcus* is the most frequent PFT in the basin (Fig. 5e), mainly in the eastern half, being twice or three fold higher than the presence of *Prochlorococcus* (Fig. 5c). However diatoms dominated in the northern Adriatic Sea and Gulf of Lions (Fig. 5g) and nanoeukaryotes presented a high frequency along the coastal fringe and the Aegean Sea (Fig. 5a). The standard deviation maps show where the variability of different PFTs is higher (Fig. 5b, d, f and h). It can be argued that unidentified pixels may represent a high percentage, but they can potentially decrease if more in situ data are included to improve the labeling step.

These spatial patterns of PFTs are in concordance with the distribution of the main taxonomic pigments estimated from the in situ HPLC dataset (Table 3). These data can be then used to visually compare the maps generated by the PHYSAT-Med method. Fig. 6 shows surface pigments ratios of divinyl Chla, zeaxanthin, fucoxanthin and 19'HF in the Mediterranean Sea over different seasons (spring, summer and autumn). The pigment ratio of divinyl Chla, which is indicative of the presence of *Prochlorococcus* (i.e. Claustre & Marty, 1995; Goericke & Repeta, 1992; Vidussi et al., 2001), exhibits low values in surface water in the entire basin, especially in summer. This finding is consistent with the distribution of *Prochlorococcus* estimated by the PHYSAT-Med method, where only a few pixels denoted this phytoplankton group (Fig. 6m, n and o). In contrast, zeaxanthin, which is diagnostic mainly for *Synechococcus* (Chisholm, 1992; Claustre & Marty, 1995; Goericke & Repeta, 1992; Guillard et al., 1985; Marty & Chiaverini, 2002; Marty et al., 2002; Vidussi et al., 2001), was found to represent the highest pigment ratio concentration throughout the year, mainly during summer, coinciding with the PHYSAT-Med outputs for the Mediterranean Sea (Figs. 4, 5 and 6). Furthermore, the in situ HPLC results indicated that fucoxanthin, which fundamentally marks the presence of diatoms (Jeffrey, 1980), presented higher values during spring and autumn and particularly in coastal areas (Alborán, Aeganan and north of the Adriatic seas), in concordance with the PHYSAT-Med distribution (Fig. 6m, n and o). Finally, maximum distributions of pigment ratio of 19'-HF (Fig. 6j, k and l) were found during spring cruises, particularly in coastal areas, coinciding with the distribution of nanoeukaryotes given by PHYSAT-Med (Fig. 6m, n and o).

In order to compare the results obtained with the two approaches considered here to estimate the pigments distribution over the Mediterranean Sea, we found 29 match-ups between pigment inventories (using thresholds of Table 4 in Alvain et al., 2005) and associated with simultaneous high quality satellite phytoplankton groups given by PHYSAT-Med ( $\text{AOT}_{865}$  lower than 0.15 and  $nLw_{555}$  lower than  $1.3 \text{ mW cm}^{-2} \text{ mm}^{-1} \text{ sr}^{-1}$ ). These validation data sets contain 16 water samples dominated by *Synechococcus* and 13 by nanoeukaryotes (Fig. 7). A synthetic view of this validation exercise is provided in Table 4 by showing, for each of these two groups, the percentage of valid and wrong identifications. Table 4 shows that 74.07% of the pigment inventories corresponding to nanoeukaryotes are associated with the same phytoplankton group in the PHYSAT-Med daily images. Moreover, *Synechococcus* are correctly identified in 60.71% of the in situ pigment inventories. In this validation exercise, the rest of the groups were discarded, as no pigment inventories in matchup were associated to them.

The temporal variability of PFTs (*Prochlorococcus*, *Synechococcus*, diatoms and nanoeukaryotes) in the Ligurian Sea (Fig. 2) was also



**Fig. 4.** Monthly climatology of the dominant phytoplankton group detected by PHYSAT-Med during the study period (July 2002–May 2013).

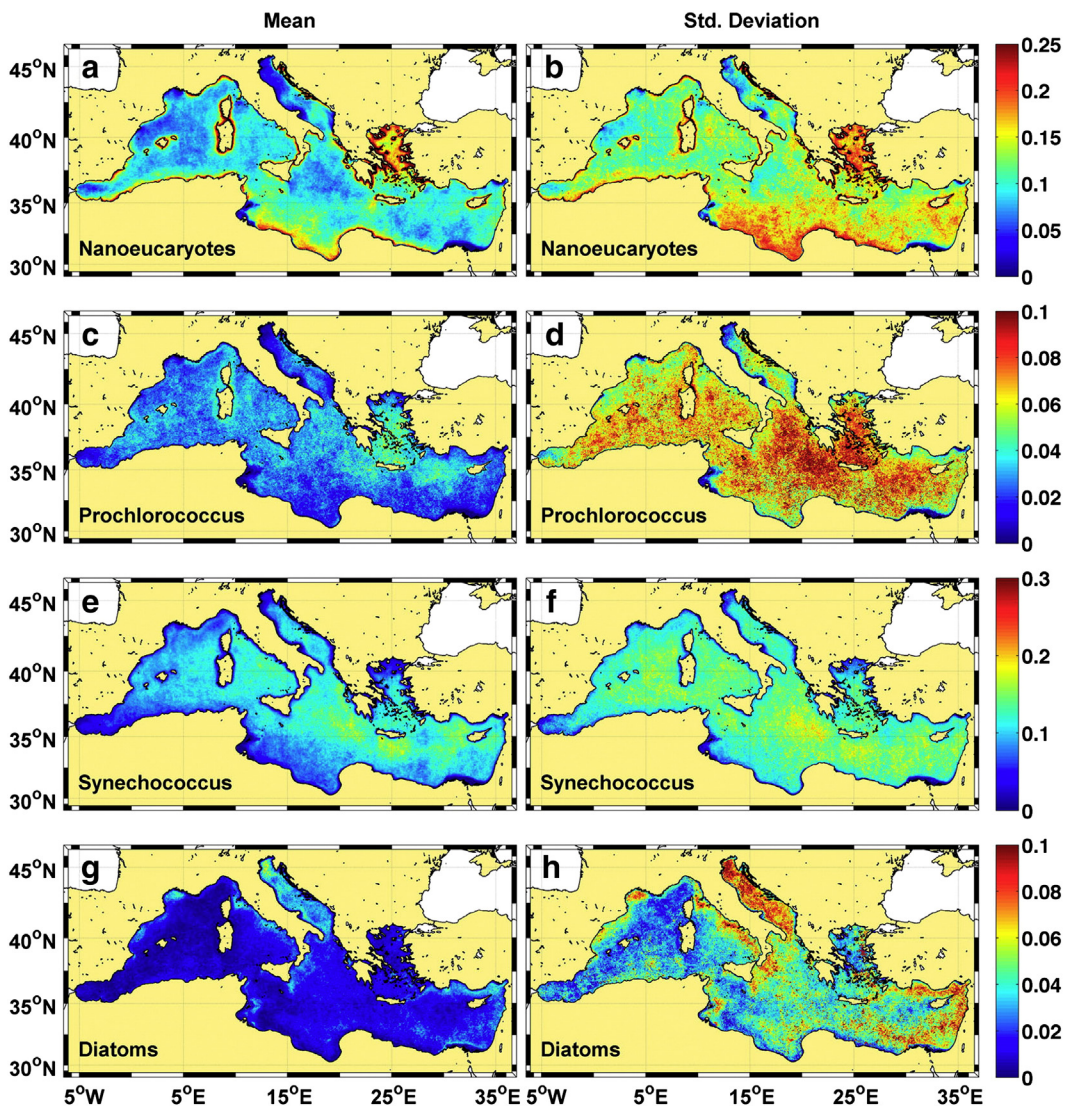


**Fig. 5.** Map of detection frequencies (0 = group never detected, 1 = all valid pixels associated with the group) during the study period for different phytoplankton groups. Left and right columns represent the mean and standard deviation, respectively. Color scale is different for each group. (For interpretation of the references to color in this figure legend, the reader is referred to the web version of this article.)

analyzed and compared with HPLC measurements (pigment ratios) provided for the same sub-basin during certain periods of time at the first optical depth. Fig. 8 shows oscillations of the four PFTs during the year, with peaks and minima appearing at different times of the year depending on the group. *Prochlorococcus* exhibited maxima at the end of the stratification period (normally in October) over several years (Fig. 8a). The maxima found by the PHYSAT-Med model were in close agreement with the maxima in the concentrations of the pigment ratio for divinyl Chl-a in the first optical depth provided by HPLC, which is indicative of prochlorophytes (Claustre & Marty, 1995; Goericke & Repeta, 1992; Vidussi et al., 2001), although this pigment ratio value is normally lower than 0.40. This pattern coincides with the results reported by Vaulot, Partensky, Neveux, Mantoura, and Llewellyn (1990) and Marty et al. (2002) estimated by flow cytometry and HPLC analysis respectively. However, during the stratification period in this region, between July and October (Marty et al., 2002), the phytoplankton group identified by PHYSAT-Med as the most abundant was *Synechococcus* (Fig. 8b). This feature also matches the highest values for zeaxanthin measured by HPLC during this period in the Ligurian Sea (Fig. 8b). As indicated above, zeaxanthin is associated with cyanobacteria (Guillard et al., 1985) and is normally used in this area to estimate *Synechococcus* concentration (Marty et al., 2002; Vidussi

et al., 2001), particularly in surface waters, where it is more abundant (Lasternas, Agustí, & Duarte, 2010). The visual concordance between the results obtained with both approaches also applies to diatoms, as the annual peaks registered by PHYSAT-Med every year during the spring bloom closely resemble the maxima of fucoxanthin given by HPLC in the first optical depth (Fig. 8c). Finally, the nanoeukaryotes present maxima during winter season, normally around January, although the maxima pigment ratio of 19'-HF is achieved during spring–summer seasons (Fig. 8d), which can be due to the heterogeneity of this phytoplankton group in terms of species composition. Therefore, the broad coincidence between both temporal patterns (Fig. 7, HPLC Pigment ratio vs PHYSAT-Med outputs) confirms in general terms that the regionalized version of PHYSAT (PHYSAT-Med) is in relatively good agreement with the results obtained by long-term monitoring programs for phytoplankton distribution, at least in the Ligurian Sea area, where the largest database of HPLC measurements is available (Table 3).

Once it has been established that PHYSAT-Med works properly in the Mediterranean Sea, the temporal and spatial variability of PFTs in different Mediterranean sub-basins have been also analyzed through this approach, and represented by the Hovmöller diagrams (Figs. 9 and 10). The transects selected to perform the analysis were quite

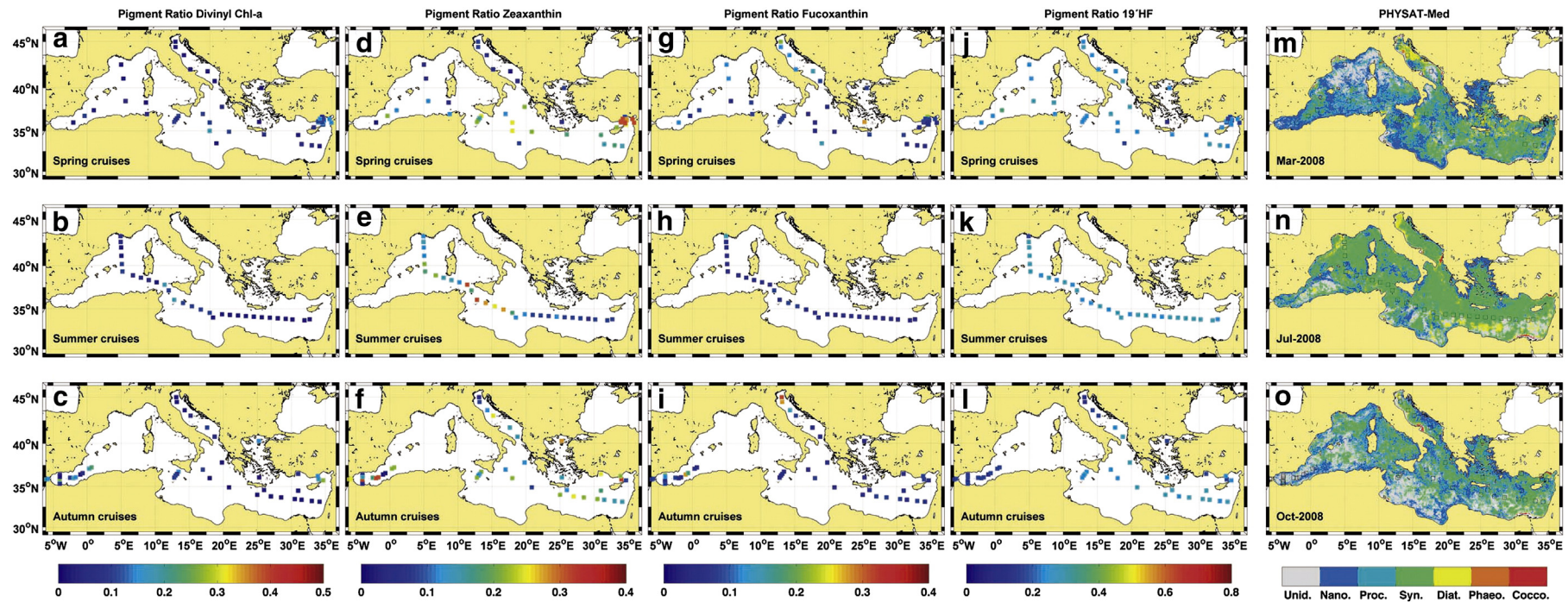


**Fig. 6.** Pigment ratio from in situ HPLC data (Table 2) averaged over the upper 35 m depth: (a, b and c) divinyl chl- $\alpha$ ; (d, e and f) zeaxanthin; (g, h and i) fucoxanthin and (j, k and l) 19'HF. Plots m, n and o display the map of the most frequent dominant phytoplankton group during March, July and October 2008, respectively.

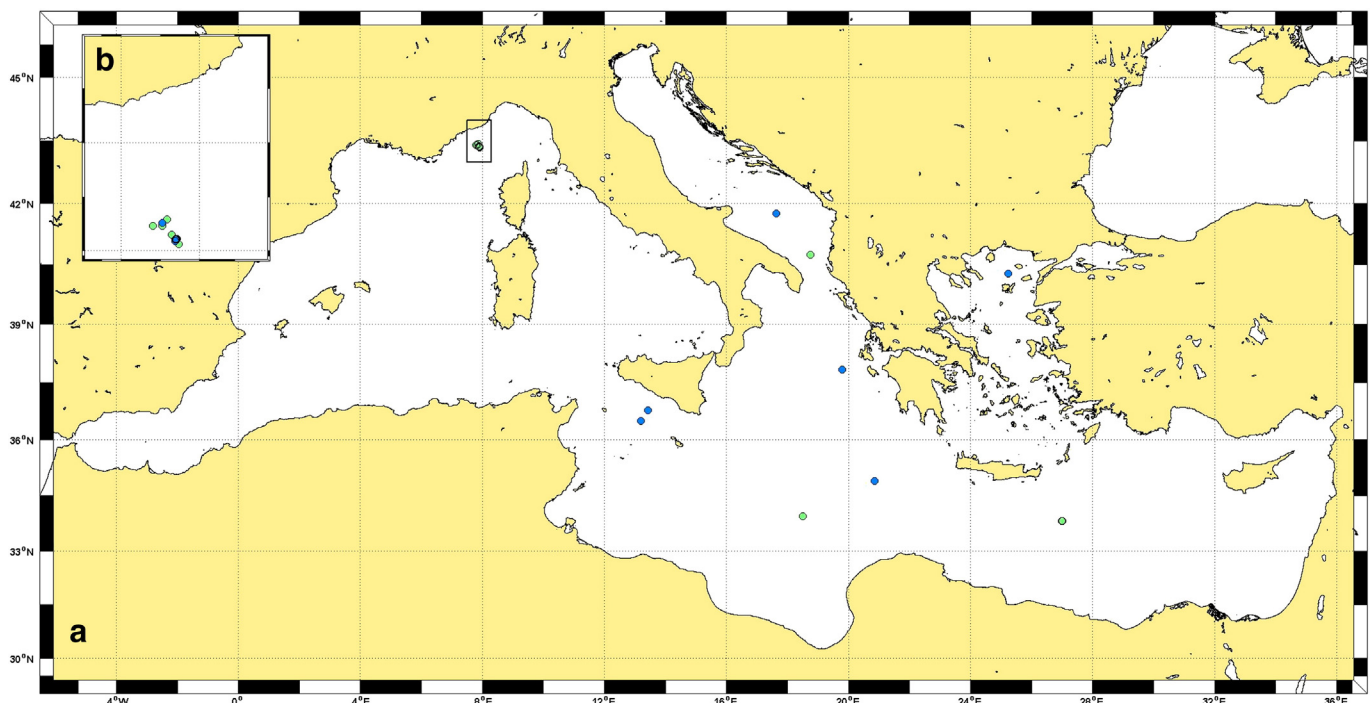


**Fig. 7.** Validation of PHYSAT-Med using HPLC in situ dataset (Table 2). Blue (nanoeukaryotes) and green (*Synechococcus*) symbols represent the location of the station where PHYSAT-Med works successfully. (For interpretation of the references to color in this figure legend, the reader is referred to the web version of this article.)

similar those used by D'Ortenzio and d'Alcalá (2009), who considered one zonal (Fig. 9) and three meridional transects (Fig. 10) that encompass the most representative areas of the chosen sub-basins (see Fig. 2 for location of the transects).

The West–East distribution of PFTs during the study period shows differences mainly between the two sub-basins. Nanoeukaryotes appear in the whole Mediterranean whereas in the Levantine basin *Synechococcus* is the most abundant group in surface waters, especially during summer (Fig. 9). This pattern can be observed every year between 2002 and 2013. On the other hand, diatoms are in general less frequent and are identified during spring, prior to the proliferation of *Synechococcus*. After the stratification period, during the autumn months, some pixels mark the prevalence of *Prochlorococcus* over the whole zonal transect whereas in winter, a large number of unidentified pixels was found, particularly in the western part of the transect. This temporal variability is also detected in the three meridional transects (Fig. 10). In all cases, the dominant group was *Synechococcus*, mostly during summer. Before the maximum, over spring, a diatom bloom can be identified in both the central and eastern transects whereas in the western transect, nanoeukaryotes emerge during winter, when many undetermined pixels were again found in the three transects. As noted previously, although unidentified pixels may represent a high percentage, this updated version of PHYSAT can still be very useful to monitor the spatio-temporal variability of some PFTs in Mediterranean Sea, as the approach can be potentially improved when more in situ measurements are incorporated.

#### 4. Discussion and conclusion

The Mediterranean Sea is generally characterized by an oligotrophy regime, with a clear decrease in nutrients and chlorophyll concentration being observed from west to east (Krom, Emeis, & Van Cappellen, 2010). However, local physical structures promoting the inputs of nutrients from the deep layer to surface water allow the formation of some productive areas that present their own dynamics within the general circulation scheme (Siokou-Frangou et al., 2010). The presence of convergences zones immersed in an oligotrophic environment and the particular biogeochemical characteristics of the Mediterranean are reflected in the composition of the phytoplankton community, whose diversity has been reported in previous studies (Siokou-Frangou et al., 2010). Given the complexity to perform large in situ studies at a basin scale, the use of novel remote tools that facilitate the monitoring the oceanic biodiversity from space (De Monte et al., 2013) represents a powerful and useful alternative approach that helps to understand phytoplankton dynamics in the Mediterranean basin.

Here, we present an updated version of the PHYSAT method (Alvain et al., 2005, 2008) that has been specifically developed for the Mediterranean Sea and for the MODIS sensors. This version, the so called PHYSAT-Med, has been compared with large in situ datasets (Tables 3 and 4, Figs. 6, 7 and 8) available for the basin. In addition, the spatio-temporal variability of the phytoplankton groups estimated by PHYSAT-Med was consistent with the previous knowledge on the phytoplankton distribution patterns in the Mediterranean Sea (Claustre & Marty, 1995; Marty & Chiaverini, 2002; Marty & Chiavérini, 2010; Marty et al., 2002; Siokou-Frangou et al., 2010; Vaulot et al., 1990; Vidussi, Marty, & Chiavérini, 2000; Vidussi et al., 2000, 2001). The concordance between the results obtained with remote data and previous in situ measurements was particularly relevant in the Ligurian Sea region (Fig. 8), where the largest database of HPLC measurements is available (Table 3).

Our results show that the temporal variability of the four phytoplankton groups discriminated by PHYSAT-Med in the Mediterranean Sea, *Synechococcus*, *Prochlorococcus*, diatoms and nanoeukaryotes can

**Table 4**

Validation results for the PHYSAT-Med method. For each group, the percentage of valid (bold) and wrong (italic) identifications are shown.

PHYSAT-MED/in situ	Nanoeukaryotes	<i>Synechococcus</i>
Nanoeukaryotes	<b>74.07</b>	39.29
<i>Synechococcus</i>	25.93	<b>60.71</b>

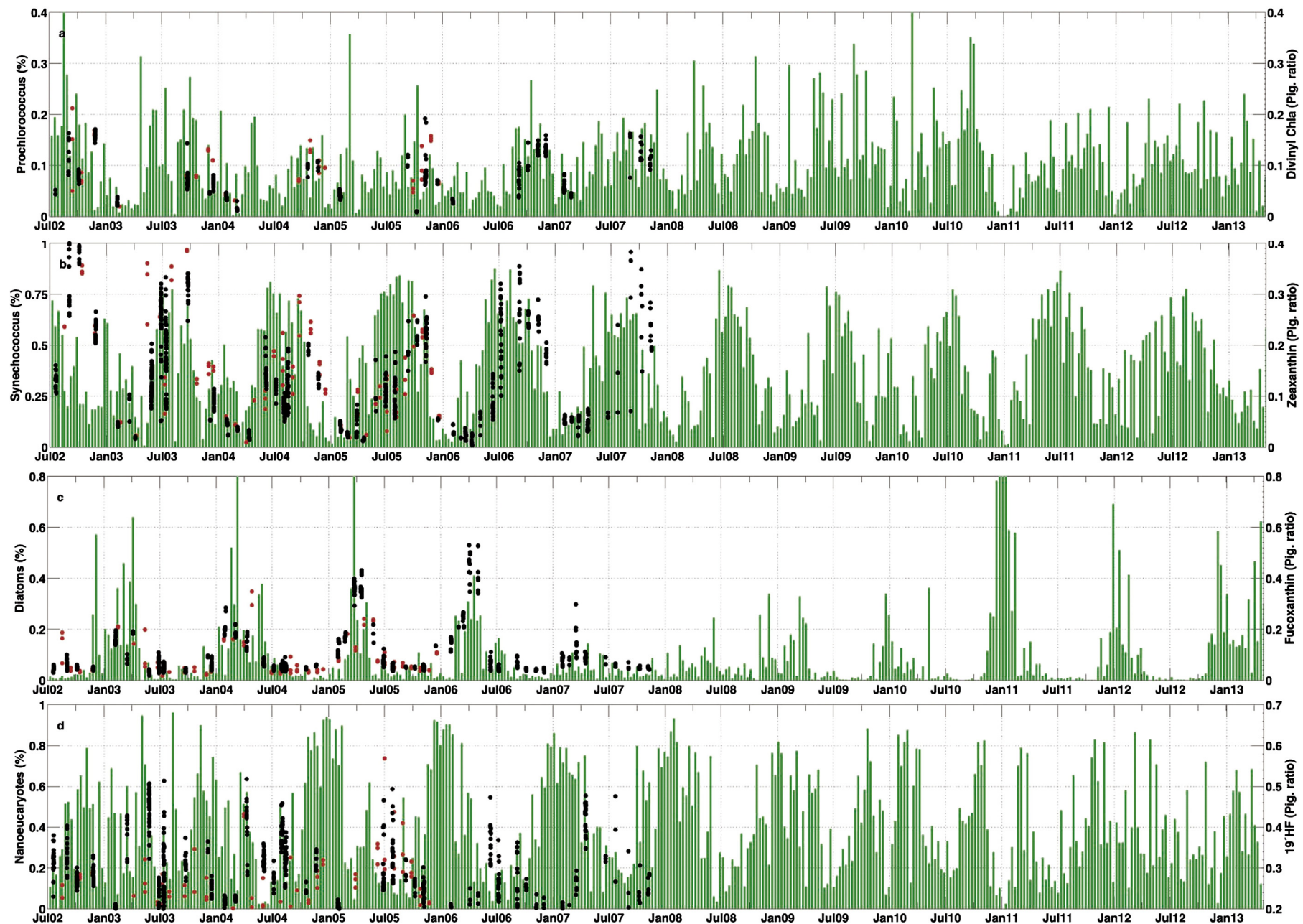


**Fig. 8.** Temporal percentage (green bars, left axis) of each phytoplankton group identified by PHYSAT-Med in the Ligurian Sea. Red and black dots (right axis) represent respectively the HPLC pigments ratio for SODYF and BOUSSOLE dataset in the first optical depth. Note that in panel d), only in situ measurements with zeaxanthin pigment ratios of >0.20 have been represented. (For interpretation of the references to color in this figure legend, the reader is referred to the web version of this article.)

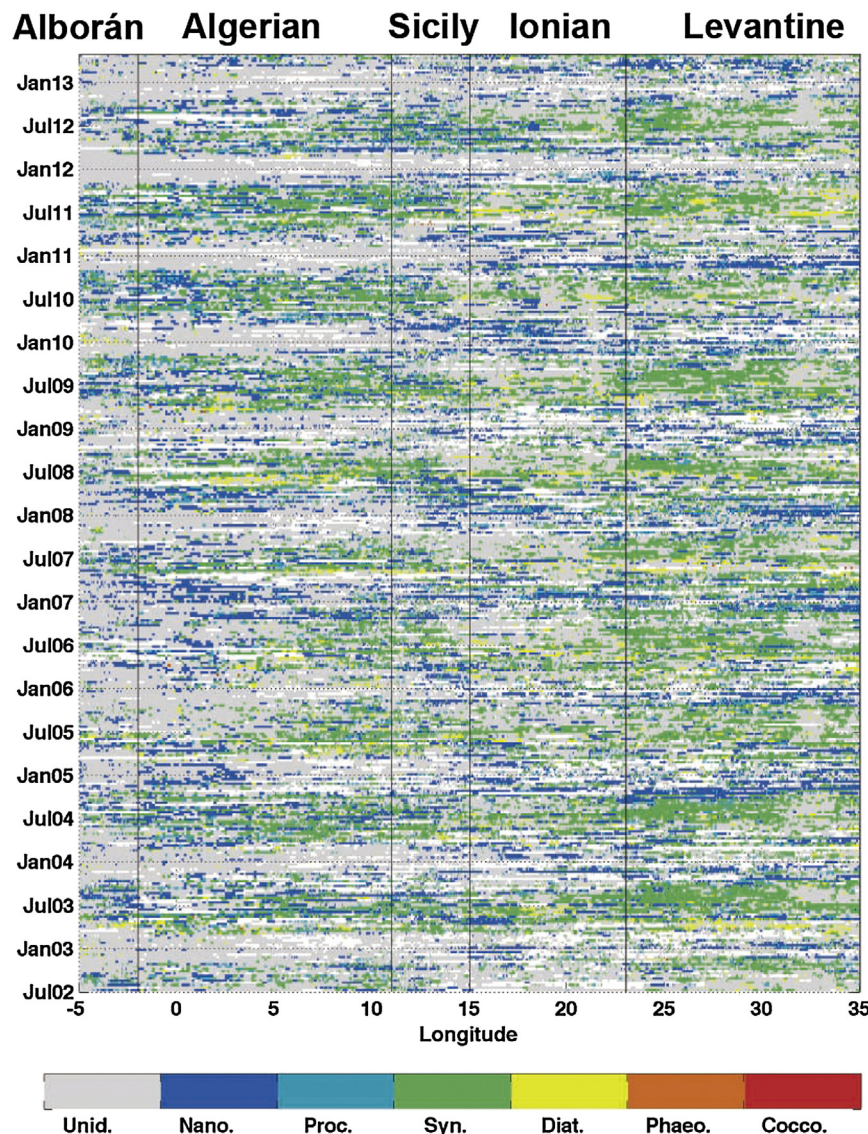


**Fig. 9.** Hoevmöller diagram on the west–east transect for the phytoplankton groups (see Fig. 1 for geographical position of the transect), which are calculated from the 10-day composite.

be reproduced (Figs. 8, 9 and 10). This enables studies of multi-scale processes, such as seasonal species' successions, interannual anomalies and decadal trends. In fact, PHYSAT has been already used successfully to analyze large-scale shifts in phytoplankton groups at a global scale (Ben Mustapha et al., 2014; Masotti et al., 2010), in the Equatorial Pacific (Masotti et al., 2011) and in high latitudes (Alvain et al., 2013; Hashioka et al., 2013), seasonal distribution of PFTs at a global scale (Alvain et al., 2008) and mesoscale patches of dominant phytoplankton groups at the confluence of the Brazil and Malvinas currents (D'Ovidio et al., 2010).

According to our study, PHYSAT-Med can be considered the first model for estimating the dynamics of the four PFTs analyzed in the Mediterranean Sea. Sathyendranath et al. (2004) proposed an algorithm to discriminate diatoms from other types of phytoplankton groups in the Northwest Atlantic, and Subramaniam et al. (2001) developed an alternative method able to detect *Trichodesmium* blooms through SeaWiFS imagery in the South Atlantic Bight. Brown and Yoder (1994) proposed an algorithm to identify coccolithophorids blooms in the global ocean, which was later used by Iglesias-Rodríguez et al. (2002) who included the Mediterranean Sea, although no specific study was dedicated to the Mediterranean Sea in spite of its particular optical and ecological character (Bricaud et al., 2002; Claustre et al., 2002; Loisel et al., 2011). Recently, Uitz, Stramski, Gentili, D'Ortenzio, and Claustre

(2012) proposed a phytoplankton class-specific bio-optical model to calculate primary production in the Mediterranean Sea, but none of these models provides the spatio-temporal distribution of different phytoplankton groups in the basin.

Furthermore, the PHYSAT-Med allowed us to include a high number of pixels in the Mediterranean by using a new LUT (Fig. 3b), which was specifically created for the basin using the regional chlorophyll *a* algorithm MedOC3-Chl-*a* (Santoleri et al., 2008). In fact, the number of pixels identified by PHYSAT-Med (Fig. 11a) is three-fold higher than that detected by the global version of PHYSAT (Alvain et al., 2005, 2008), being also in agreement with in situ HPLC measurements at the Ligurian sub-basin (i.e. diatoms, Fig. 11b). Recently, Ben Mustapha et al. (2014) applied modified PHYSAT approach (PHYSAT-SOM) at global scale, which provides a much higher number of pixels (twice as high) than the previous PHYSAT version.

The comparison exercise performed here shows consistent results for the Ligurian Sea region. In this sub-basin, the seasonal succession of hydrological conditions induces production regimes varying from mesotrophy in spring to oligotrophy in summer and fall (Marty et al., 2002). The winter convective-mixing period that extends from the beginning of December to the end of March (Marty et al., 2002) allows the replenishment of nutrient in the surface layers, which supports

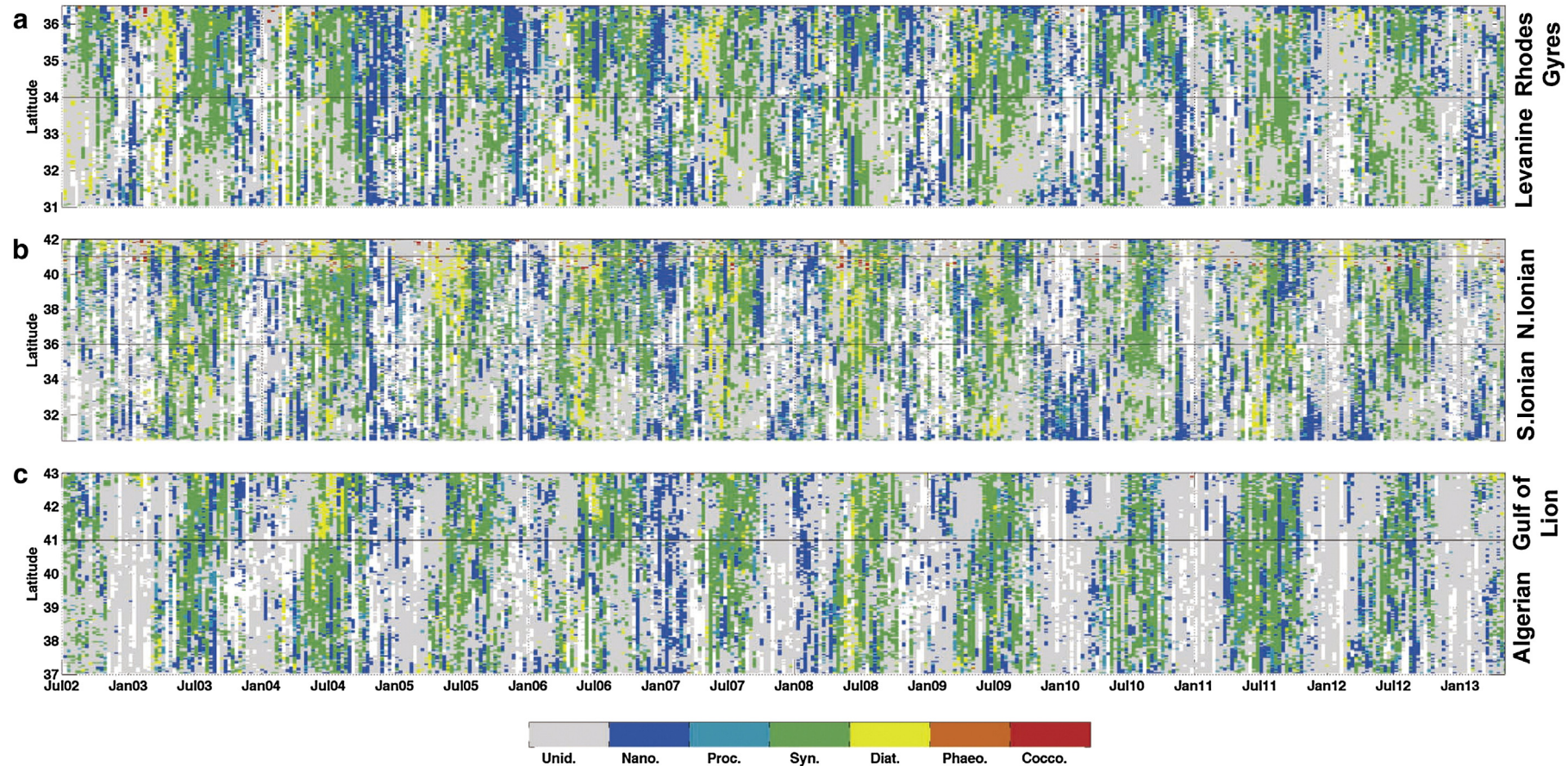


**Fig. 10.** Hoevmoeller diagram on the north–south transects of the phytoplankton groups (see Fig. 1 for geographical position of the transect), which are calculated from the 10-day composite. (a) Levantine basin, (b) central Mediterranean and (c) western Mediterranean.

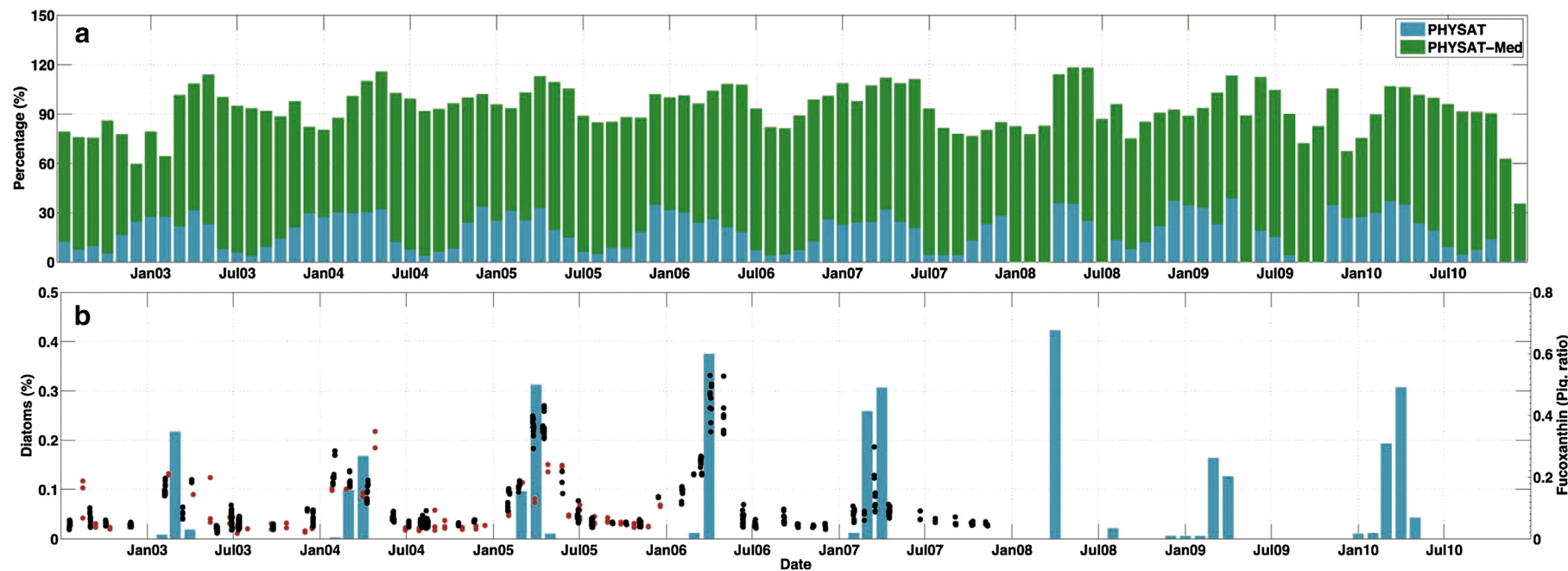


**Fig. 11.** (a) Monthly time series of the percentage of pixels of PFT identified by PHYSAT-Med (green bars) and PHYSAT (cyan bars). (b) Temporal percentage (cyan bars, left axis) of diatom group identified by PHYSAT (Alvain et al., 2005, 2008) in the Ligurian Sea. Red and black symbols (right axis) represent the fucoxanthin pigment ratio for SODYF and BOUSSOLE datasets respectively in the first optical depth. PHYSAT Global data can be downloaded from the website: <http://log.univ-littoral.fr/Physat>. (For interpretation of the references to color in this figure legend, the reader is referred to the web version of this article.)

phytoplankton new production (Marty & Chiavérini, 2010). According to the PHYSAT-Med outputs (Fig. 12), nanoeukaryotes were the dominant phytoplankton group during the winter months, whereas diatoms achieved a maximum during the spring bloom in this area (Figs. 8c and 12), coinciding with the maximum in chlorophyll *a* concentration measured in situ (Marty & Chiavérini, 2010; Marty et al., 2002). Diatoms are known to be opportunistic organisms (Fogg, 1991) that take advantage of the newly available nutrients after the winter mixing. The seasonal variations in diatoms obtained by PHYSAT-Med (Fig. 8c) were obvious and markedly repetitive from year to year, in agreement with previous results (Marty et al., 2002). Moreover, diatoms also occur in winter–spring in other sub-basins, such as the Adriatic and Ionian seas (Fig. 4 and Supplementary material). Therefore, the geographic pattern obtained by satellite data was consistent with the previous knowledge of phytoplankton communities' organization in these regions (Caroppo, Turicchia, & Margheri, 2006; Socal et al., 1999).

After decay of the spring bloom in the Ligurian Sea, the warming of surface waters causes a rapid stabilization of the surface layer, which increases in depth from June to October (Marty & Chiavérini, 2010). During the stratification period, *Synechococcus* was found to be the most abundant group by PHYSAT-Med (Figs. 4, 8 and 11), coinciding with the maxima concentration of zeaxanthin (*Synechococcus*) measured in the surface layers by Marty and Chiaverini (2002). This period also corresponds to a shift from a phytoplankton population dominated by diatoms (Figs. 8, 10 and 12) toward an increase in cyanobacteria (*Synechococcus*). Marty et al. (2002) established that the maximum contribution of cyanobacteria-characteristic pigment (zeaxanthin) occurs in summer and in surface waters, which is also the period of phosphate limitation. During the winter mixing, nutrient limitation is essentially due to nitrate depletion in surface waters (where most of the productivity proceeds). Marty and Chiaverini (2002) suggested that this increase could be due to the better efficiency for cyanobacteria to grow under nutrient limited conditions, either by atmospheric nitrogen fixation or by utilization of atmospheric deposition of nutrient-aerosols or rain, which are relevant fertilization processes in the Mediterranean nutrient cycling (Huertas et al., 2012). Our data confirm that maxima in *Synechococcus* distribution are achieved during the stratification period (Fig. 12), which is unequivocally detected during this season every year (Fig. 8b). Zeaxanthin, a pigment that likely acts as a photo-protector (Paerl, Tucker, & Bland, 1983), is particularly

abundant in the surface layer during the nutrient-depleted stratification period. The abundance of cyanobacteria-associated zeaxanthin in the upper layers can be attributed to a photosynthetic adaptation resulting from changes in their phycobiliprotein concentrations at high irradiances (Kana & Glibert, 1987). However, it is also consistent with their potential capability to fix atmospheric nitrogen, as already suggested for *Synechococcus* (Mitsui et al., 1986; Sachs & Repeta, 1999). The presence of *Synechococcus* is particularly important in the Eastern Mediterranean during 2003 and the rest of years analyzed (Supplementary material). Its distribution, specifically restricted to surface layers, is consistent with data reported in other Mediterranean sub-basins, such as the Tyrrhenian Sea (Decembrini, Caroppo, & Azzaro, 2009), Ionian Sea (Brunet et al., 2006; Casotti et al., 2003), Ligurian Sea (Bustillo-Guzman, Claustre, & Marty, 1995), Adriatic Sea (Santic, Krstulovic, Solic, & Kuspilic, 2011) and in surface coastal water of the northwestern Mediterranean Sea (Sommaruga, Hofer, Alonso-Saez, & Gasol, 2005).

On the contrary, *Synechococcus* abundance markedly decreases during the destratification period that begins in November, when mixing starts and triggers nutrients inputs to the surface layer. High divinyl Chl-*a*, which is the marker for *Prochlorococcus* (i.e. Goericke & Repeta, 1992), concentrations have been measured from summer to winter but remain undetectable the rest of the year (Marty et al., 2002). This pattern is corroborated by data plotted in Fig. 8a, where the divinyl Chl-*a* in the first optical depth peaks between October and December, coinciding with *Prochlorococcus* maxima given by PHYSAT-Med (Fig. 8a). In any case, our data indicates that *Synechococcus* is more abundant than *Prochlorococcus* at any time of the year, in agreement with the study carried out by Schauer, Balagué, Pedrós-Alió, and Massana (2003). This finding would be also coherent with the oligotrophic character of the Eastern Mediterranean, at least during the destratification period. In addition, our data indicate that prochlorophytes (Fig. 4 and Supplementary material) are generally less abundant in the northwestern Mediterranean Sea than in the south-eastern, in agreement with previous observations (Barlow, Mantoura, Cummings, & Fileman, 1997; Vidussi et al., 2000). Nevertheless, it should be pointed out that *Prochlorococcus* mostly thrives in deeper layers, particularly at the deep chlorophyll maximum (Lasternas et al., 2010; Mella-Flores et al., 2010) and hence, it would not be detect by PHYSAT-Me, which is suitable for identification of PFTs in the surface layer (first optical depth).

Our study then evidences that PHYSAT-Med data matches in situ picoplankton abundance and dynamics in the Mediterranean, at least in surface and for *Prochlorococcus* and *Synechococcus*. This concordance can be extended in the case of nanoeukaryotes. Thus, Vidussi et al. (2001) found that nanophytoplankton always prevailed over picoplankton in the Ionian Sea during winter months and Uitz et al. (2012) proposed that primary production was dominated by nanophytoplankton throughout the year in the entire basin. The distribution of nanoeukaryotes given by PHYSAT-Med (i.e. year 2004, Supplementary material) is also in agreement with such observations, with this pattern being particularly evident in the Aegean Sea. In contrast, Vidussi et al. (2001) also noted that picoplankton was dominant in the Levantine basin, which was confirmed by our satellite data (i.e. year 2004 in Supplementary material). PHYSAT-Med may have, however, certain limitations to detect other phytoplankton groups. This is the case of diatoms, which may present two spectral behaviors in terms of shape and amplitude (Ben Mustapha et al., 2014) and therefore its distribution in the Mediterranean Sea would be underestimated by the current approach.

This constrain can be also applied to coccolithophorids. PHYSAT-Med generated maps (Fig. 4 and Supplementary material) indicated that coccolithophorids were mainly located along the Mediterranean coastline, particularly in the vicinity of large rivers mouths, such as Nile, Ebro, Rhone and Adriatic Sea. However, it can be argued that the observed patches could be well due to the presence of terrestrial matter and/or a specific phytoplankton group not yet sampled. In addition, coccolithophorids occurrence has been described globally at the Mediterranean (Coll et al., 2010; Cros & Fortuno, 2002; Oviedo, Ziveri, Alvarez, & Tanhua, 2014)

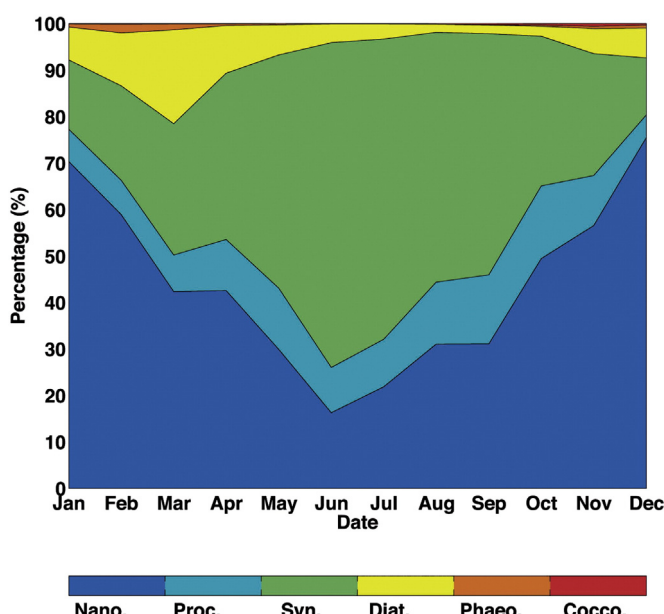


Fig. 12. Monthly climatological mean of the seasonal cycle of the percentage of each phytoplankton group in the Ligurian Sea during 2003–2012 period.

whereas PHYSAT-Med outputs only marked a few pixels where this group was clearly represented (Fig. 4 and Supplementary material). Such disparity could be related to the use of a mask for turbid pixels that were defined by  $nLW_{555} > 1.3 \text{ mW cm}^{-2} \text{ mm}^{-1} \text{ sr}^{-1}$  (Nezlin & DiGiocomo, 2005), leading to an overestimation of this group. It has been reported that suspended sediments having a calcareous composition can also mimic coccolithophorids blooms (Brown & Podestá, 1997). All these factors highlight that the identification of coccolithophores by remote sensing is not straight forward (Nair et al., 2008), even though in the literature there are several algorithms already in use to identify this phytoplankton group from space, which are generally based on retrieval of the backscattering coefficient and the estimation of the calcite concentration via empirical relationship (Ackleson et al., 1994; Brown & Podestá, 1997; Brown & Yoder, 1994; Cokacar et al., 2001; Gordon et al., 2001; Iglesias-Rodríguez et al., 2002; Kopelevich et al., 2013; Moore et al., 2012; Smyth et al., 2002; Tyrell et al., 1999).

Similarly, even though PHYSAT-Med can be also applied to detect "Phaeocystis-like" group, no signals were found in our study. Since *Phaeocystis* is a genus with a worldwide distribution (Schoemann, Becquevort, Stefels, Rousseau, & Lancelot, 2005), including the Mediterranean Sea (Zingone, Chrétiennot-Dinet, Lange, & Medlin, 1999), it is then clear that is possible that more in situ information will allow to support others anomalies' labeling in the future. In fact, *Phaeocystis*-like groups were initially included in formulation of PHYSAT-v2008 method (Alvain et al., 2008) based on coherent specific spatial structures associated to this group available in the literature, but a more powerful validation against in situ observations is needed to mark the presence of this group from space, at least in the Mediterranean. This would be case of other specific phytoplankton groups occurring in the Mediterranean Sea could be well added to PHYSAT-Med in the future, when extensive and accurate in situ data about on their abundance allow calibration and validation of the method. For instance, dinoflagellates occur widely across the Mediterranean Sea (Coll et al., 2010; Gómez, 2003) but in situ measurements have not been taken into account in the present first attempt to compute a PHYSAT-Med version.

Recent studies have also shown that well marked mixed situation could be theoretically detected by the PHYSAT approach (Alvain et al., 2012). As indicated above, the shape and amplitude of the Ra spectra mainly depend on the bio-optical environment, represented by different values of  $b_p$ ,  $a_{cdom}$  and  $a_{phy}$ . As shown by those authors, the  $a_{cdom}$  strongly controls the spectral shape of Ra in the blue part of the spectrum. For low  $a_{cdom}$  values, the Ra spectra decrease from the blue to red wavelengths, while they increase with the wavelengths for high  $a_{cdom}$  values. For  $a_{phy}$ , the highest Ra sensitivity is found at 443 nm. The  $b_p$  has a restricted effect on the spectral shape but represents the main factor affecting the Ra absolute values at all the wavelengths.

In conclusion, PHYSAT-Med provides us a regionalized algorithm to estimate dominant phytoplankton groups (nanoeukaryotes, *Prochlorococcus*, *Synechococcus*, diatoms, coccolithophorids and *Phaeocystis*-like) in the first optical depth of the Mediterranean Sea. The comparison exercise performed here using in situ HPLC datasets and previous measurements shows a reasonable visual agreement for four groups, *Prochlorococcus*, *Synechococcus*, nanoeukaryotes and diatoms. Our study evidences the dominance of *Synechococcus* over prochlorophytes throughout the year, whereas nanoeukaryotes were more abundant during winter months. However, diatoms seemed to augment during the spring period (March to April), especially in the Ligurian and Adriatic seas. It is clear that data analysis through PHYSAT-Med provides hints only on the most abundant phytoplankton types and in the surface layer but it could be still considered a useful tool for monitoring the dynamics and maintenance of planktonic biodiversity in the Mediterranean. Satellite information on the phytoplankton groups distribution can be used for a better estimate of Chla concentration (Alvain et al., 2006) in the Mediterranean Sea where standard bio-optical algorithms display a considerable bias (Bosc, Bricaud, & Antoine, 2004; Bricaud et al., 2002; D'Ortenzio & d'Alcalá, 2002; Morel & Gentili,

2009; Santolieri et al., 2008; Volpe et al., 2007). PHYSAT-Med could potentially be also used to verify PFTs in ecological models, as the lack of in situ phytoplankton groups data is regarded as a major problem in phytoplankton ecosystem modeling (Anderson, 2005). Our approach should be then understood as the first version of an algorithm susceptible to be completed when more in situ measurements allow validation for other phytoplankton groups that, at the moment, could not be included in the method formulation.

## Acknowledgments

This research was supported by the PERSEUS European Project and PR11-RNM-7722 Andalucía Regional Project. The authors acknowledge the NASA/GSFC/DAAC for providing access to L3 MODIS products. In situ HPLC dataset was obtained from SESAME EU Project, BOUSSOLE Project and MAREDAT data. We thank J. Ras and the members of the SAPIGH analytical platform from the *Laboratoire d'Océanographie de Villefranche* for the HPLC analysis. GN was supported by the program "Salvador Madariaga, Ministerio de Educación, Cultura y Deporte, Programa Nacional de Movilidad de Recursos Humanos del Plan Nacional de I-D + i 2008–2011, prorrogado por Acuerdo de Consejo de Ministros de 7 de octubre de 2011".

## Appendix A. Supplementary data

Supplementary data to this article can be found online at <http://dx.doi.org/10.1016/j.rse.2014.06.029>.

## References

- Ackleson, S. G., Balch, W. M., & Holligan, P.M. (1994). Response of water-leaving radiance to particulate calcite and chlorophyll a concentrations: A model for Gulf of Maine coccolithophore blooms. *Journal of Geophysical Research*, *99*, 7483–7499.
- Aiken, J., Pradhan, Y., Barlow, R., Lavender, S., Poulton, A., Holligan, P., et al. (2009). Phytoplankton pigments and functional types in the Atlantic Ocean: A decadal assessment, 1995–2005. AMT Special Issue. *Deep-Sea Research II*, *56*, 899–917.
- Alvain, S., Le Quéré, C., Bopp, L., Racault, M. F., Beaugrand, G., Dessailly, D., et al. (2013). Rapid climatic driven shifts of diatoms at high latitudes. *Remote Sensing of Environment*, *132*, 195–201.
- Alvain, S., Loisel, H., & Dessailly, D. (2012). Theoretical analysis of ocean color radiances anomalies and implications for phytoplankton groups detection in case 1 waters. *Optics Express*, *20*, 2.
- Alvain, S., Moulin, C., & Dandonneau, Y. (2008). Seasonal distribution and succession of dominant phytoplankton groups in the global ocean: A satellite view (SeaWiFS 1998–2006). *Global Biogeochemical Cycles*, *22*.
- Alvain, S., Moulin, C., Dandonneau, Y., & Breon, F. M. (2005). Remote sensing of phytoplankton groups in case 1 waters from global SeaWiFS imagery. *Deep-Sea Research I*, *1*, 1989–2004.
- Alvain, S., Moulin, C., Dandonneau, Y., Loisel, H., & Bréon, F. M. (2006). A species-dependent bio-optical model of case I waters for global ocean color processing. *Deep Sea Research, Part I*, *53*, 917–925.
- Anderson, T. R. (2005). Plankton functional type modelling: Running before we can walk? *Journal of Plankton Research*, *27*, 1073–1081.
- Antoine, D., Chami, M., Claustre, H., D'Ortenzio, F., Morel, A., Béchu, G., et al. (2006). BOUSSOLE: A joint CNRS-INSU, ESA, CNES and NASA ocean color calibration and validation activity. NASA Technical memorandum No. 2006214147, (61 pp.).
- Antoine, D., Morel, A., & Andre, J. (1995). Algal pigment distribution and primary production in the eastern Mediterranean as derived from Coastal Zone Color Scanner observations. *Journal of Geophysical Research*, *100*, 16193–16209.
- Arin, L., Morán, X. A. G., & Estrada, M. (2002). Phytoplankton size distribution and growth rates in the Alboran Sea (SW Mediterranean): Short term variability related to meso-scale hydrodynamics. *Journal of Plankton Research*, *24*, 1019–1033.
- Arnold, S. R., Spracklen, D.V., Gebhardt, S., Custer, T., Williams, J., Peeken, I., et al. (2010). Relationships between atmospheric organic compounds and air-mass exposure to marine biology. *Environmental Chemistry*, *7*, 232–241.
- Astoreca, R., Rousseau, V., Ruddick, K., Knechiak, C., Van Mol, B., Parent, J. Y., et al. (2009). Development and application of an algorithm for detecting *Phaeocystis globosa* blooms in the Case 2 Southern North Sea waters. *Journal of Plankton Research*, *31*, 287–300.
- Barlow, R. G., Mantoura, R. F. C., Cummings, D.G., & Fileman, T. W. (1997). Pigment chemotaxonomic distributions of phytoplankton during summer in the western Mediterranean. *Deep-Sea Research Part II*, *44*, 833–850.
- Belviso, S., Masotti, I., Tagliabue, A., Bopp, L., Brockmann, P., Fichot, C., et al. (2012). DMS dynamics in the most oligotrophic subtropical zones of the global ocean. *Biogeochemistry*, *110*, 215–241.
- Ben Mustapha, Z., Alvain, S., Jamet, C., Loisel, H., & Dessailly, D. (2014). Automatic classification of water-leaving radiance anomalies from global SeaWiFS imagery:

- Application to the detection of phytoplankton groups in open ocean waters. *Remote Sensing of Environment*, 146 (97–12).
- Bopp, L., Aumont, O., Cadule, P., Alvain, S., & Gehlen, M. (2005). Response of diatoms distribution to global warming and potential implications: A global model study. *Geophysical Research Letters*, 32 L19606.
- Bosc, E., Bricaud, A., & Antoine, D. (2004). Seasonal and interannual variability in algal biomass and primary production in the Mediterranean Sea, as derived from 4 years of SeaWiFS observations. *Global Biogeochemical Cycles*, 18, <http://dx.doi.org/10.1029/2003GB002034>.
- Brewin, R. J., Sathyendranath, S., Hirata, T., Lavender, S. J., Barciela, R. M., & Hardman-Mountford, N. J. (2010). A three-component model of phytoplankton size class for the Atlantic Ocean. *Ecological Modelling*, 221, 1472–1483.
- Bricaud, A., Bosc, E., & Antoine, D. (2002). Algal biomass and sea surface temperature in the Mediterranean basin. Intercomparison of data from various satellite sensors, and implications for primary production estimates. *Remote Sensing of Environment*, 81, 163–178.
- Brown, C. W., & Podestá, G. P. (1997). Remote sensing of coccolithophore blooms in the Western South Atlantic Ocean. *Remote Sensing of Environment*, 60, 83–91.
- Brown, C. W., & Yoder, J. A. (1994). Coccolithophorid blooms in the global ocean. *Journal of Geophysical Research*, 99, 7467–7482.
- Brunet, C., Casotti, R., Vantrepotte, V., Corato, F., & Conversano, F. (2006). Picophytoplankton diversity and photoacclimation in the Strait of Sicily (Mediterranean Sea) in summer. I. Mesoscale variations. *Aquatic Microbial Ecology*, 44, 127–141.
- Bustillos-Guzmán, J., Claustré, H., & Marty, J. C. (1995). Specific phytoplankton signatures and their relationship to hydrographic conditions in the coastal northwestern Mediterranean Sea. *Marine Ecology Progress Series*, 124, 247–258.
- Caroppo, C., Turicchia, S., & Margheri, M. C. (2006). Phytoplankton assemblages in coastal waters of the northern Ionian Sea (eastern Mediterranean), with special reference to cyanobacteria. *Journal of the Marine Biological Association of the United Kingdom*, 86, 927–937.
- Casotti, R., Landolfi, A., Brunet, C., D'Ortenzio, F., Mangoni, O., d'Alcalà, Ribera M., et al. (2003). Composition and dynamics of the phytoplankton of the Ionian Sea (eastern Mediterranean). *Journal Geophysical Research*, 108.
- Chisholm, S. W. (1992). Phytoplankton size. In P. G. Falkowski, & A.D. Woodhead (Eds.), *Primary productivity and biogeochemical cycles in the sea* (pp. 213–217). New York: Plenum.
- Ciotti, A., & Bricaud, A. (2006). Retrievals of a size parameter for phytoplankton and spectral light absorption by Colored Detrital Matter from water-leaving radiances at SeaWiFS channels in a continental shelf region off Brazil. *Limnology and Oceanography: Methods*, 4, 237–253.
- Claustré, H., & Marty, J. C. (1995). Specific phytoplankton biomasses and their relation to primary production in the Tropical North Atlantic. *Deep-Sea Research Part I*, 42, 1475–1493.
- Claustré, H., Morel, A., Hooker, S. B., Babin, M., Antoine, D., Oubelkheir, K., et al. (2002). Is desert dust making oligotrophic waters greener? *Geophysical Research Letters*, 29(10), 1469.
- Cokcar, T., Kubilay, N., & Oguz, T. (2001). Structure of *E. huxleyi* blooms in the Black Sea surface waters as detected by SeaWiFS imagery. *Geophysical Research Letters*, 28, 4607–4610.
- Coll, M., Piroddi, C., Steenbeek, J., Kaschner, K., Ben Rais Lasram, F., et al. (2010). The biodiversity of the Mediterranean Sea: Estimates, patterns, and threats. *PLOS ONE*, 5(8), e11842, <http://dx.doi.org/10.1371/journal.pone.0011842>.
- Cros, L., & Fortuno, J. M. (2002). Atlas of northwestern Mediterranean coccolithophores. *Scientia Marina*, 66, 7–182.
- D'Ortenzio, F., & d'Alcalà, Ribera M. (2009). On the trophic regimes of the Mediterranean Sea: A satellite analysis. *Biogeosciences*, 6, 139–148.
- D'Ovidio, F., De Monte, S., Alvain, S., Dandonneau, Y., & Levy, M. (2010). Fluid dynamical niches of phytoplankton types. *Proceeding of the National Academy of Sciences of the United States of America*, 107(43), 18366–18370.
- Dandonneau, Y., Montel, Y., Blanchot, J., Giraudieu, J., & Neveux, J. (2006). Temporal variability in phytoplankton pigments, picoplankton and coccolithophores along a transect through the North Atlantic and tropical southwestern Pacific. *Deep Sea Research Part I: Oceanographic Research Papers*, 53, 689–712.
- De Monte, S., Socodato, A., Alvain, S., & d'Ovidio, F. (2013). Can we detect oceanic biodiversity hotspots from space? *The ISME Journal*, 1–3, <http://dx.doi.org/10.1038/ismej.2013.72>.
- Decembrini, F., Caroppo, C., & Azzaro, M. (2009). Size structure and production of phytoplankton community and carbon pathways channelling in the Southern Tyrrhenian Sea (Western Mediterranean). *Deep Sea Research Part II: Topical Studies in Oceanography*, 56, 687–699.
- Demarcq, H., Reygondeau, G., Alvain, S., & Vantrepotte, V. (2012). Monitoring marine phytoplankton seasonality from space. *Remote Sensing of Environment*, 117, 211–222.
- D'Ortenzio, F., Marullo, S., Ragni, M., d'Alcalà, Ribera M., & Santoleri, R. (2002). Validation of empirical SeaWiFS algorithms for chlorophyll-a retrieval in the Mediterranean Sea: A case study for oligotrophic seas. *Remote Sensing of Environment*, 82, 79–94.
- Flecha, S., Pérez, F. F., Navarro, G., Ruiz, J., Olivé, I., Rodríguez-Gálvez, S., et al. (2012). Anthropogenic carbon inventory in the Gulf of Cádiz. *Journal of Marine Systems*, 92, 67–75.
- Fogg, G. E. (1991). The phytoplanktonic ways of life. *New Phytologist*, 118, 191–232.
- Gieskes, W. W. C., & Kraay, G. W. (1983). Dominance of Cryptophyceae during the phytoplankton spring bloom in the central North Sea detected by HPLC analysis of pigments. *Marine Biology*, 75, 179–185.
- Gieskes, W. W. C., Kraay, G. W., Nontji, A., Setiapermana, D., & Sutomo, D. (1988). Monsoonal alternation of a mixed and a layered structure in the phytoplankton of the euphotic zone of the Banda Sea (Indonesia): A mathematical analysis of algal pigment fingerprints. *Netherlands Journal of Sea Research*, 22, 123–137.
- Goericke, R., & Repeta, D. (1992). The pigments of *Prochlorococcus marinus*: The presence of divinyl-chlorophylls a and b in a marine prokaryote. *Limnology and Oceanography*, 37, 425–433.
- Goericke, R., & Repeta, D. (1993). Chlorophylls a and b and divinyl chlorophylls a and b in the open subtropical North Atlantic Ocean. *Marine Ecology Progress Series*, 101, 307–313.
- Gómez, F. (2003). Checklist of Mediterranean free-living dinoflagellates. *Botanica Marina*, 46, 215–242.
- Gordon, H. R., Boynton, G. C., Balch, W. M., Groom, S. B., Harbour, D. S., & Smyth, T. J. (2001). Retrieval of coccolithophore calcite concentration from SeaWiFS imagery. *Geophysical Research Letters*, 28(8), 1587–1590.
- Gorgues, T., Menkes, C., Slemons, L., Aumont, O., Dandonneau, Y., Radenac, M. H., et al. (2010). Revisiting the La Niña 1998 phytoplankton blooms in the equatorial Pacific. *Deep Sea Research Part I: Oceanographic Research Papers*, 57, 567–576.
- Guillard, R. R. L., Murphy, L. S., Foss, P., & Liaen-Jensen, S. (1985). *Synechococcus* spp. as likely zeaxanthin-dominant ultraphytoplankton in the North Atlantic. *Limnology and Oceanography*, 30, 412–414.
- Hashioka, T., Vogt, M., Yamanaka, Y., Le Quéré, C., Buitenhuis, E. T., Aita, M. N., et al. (2013). Phytoplankton competition during the spring bloom in four plankton functional type models. *Biogeosciences*, 10, 6833–6850.
- Hirata, T., Hardman-Mountford, N. J., Barlow, R., Lamont, T., Brewin, R., Smyth, T., et al. (2009). An inherent optical property approach to the estimation of size-specific photosynthetic rates in eastern boundary upwelling zones from satellite ocean colour: An initial assessment. *Progress in Oceanography*, 83, 393–397.
- Huertas, I. E., Ríos, A. F., García-Lafuente, J., Navarro, G., Makouï, A., Sánchez-Román, A., et al. (2012). Atlantic forcing of the Mediterranean oligotrophy. *Global Biogeochemical Cycles*, 26, GB2022, <http://dx.doi.org/10.1029/2011GB004167>.
- Iglesias-Rodríguez, M. D., Brown, C. W., Doney, S. C., Kleypas, J., Kolber, D., Kolber, Z., et al. (2002). Representing key phytoplankton functional groups in ocean carbon cycle models: Coccolithophorids. *Global Biogeochemical Cycles*, 16, 1100.
- Ignatiades, L., Gotsis-Skretas, O., Pagou, K., & Krasakopoulou, E. (2009). Diversification of phytoplankton community structure and related parameters along a large-scale longitudinal east–west transect of the Mediterranean Sea. *Journal of Plankton Research*, 31, 411–428.
- Jeffrey, S. W. (1980). Algal pigment systems. In P. Falkowski (Ed.), *Primary productivity in the sea* (pp. 33–58). New York: Plenum Press.
- Jeffrey, S. W. (1997). Application of pigment methods to oceanography. In S. W. Jeffrey, R. F. C. Mantoura, & S. W. Wright (Eds.), *Phytoplankton pigments in oceanography* (pp. 127–178). Paris: UNESCO.
- Jeffrey, S. W., & Hallegraeff, G. M. (1987). Phytoplankton pigments, species and light climate in a complex warm-core eddy of the East Australian Current. *Deep Sea Research Part A Oceanographic Research Papers*, 34, 649–673.
- Jeffrey, S. W., & Veski, M. (1997). Introduction to marine phytoplankton and their pigment signatures. In S. W. Jeffrey, R. F. C. Mantoura, & S. W. Wright (Eds.), *Phytoplankton pigments in oceanography* (pp. 407–428). Paris: U.N. Educ., Sci., and Cult. Org.
- Kana, T. M., & Gilbert, P. M. (1987). Effect of irradiances up to 2000 mE s<sup>-1</sup> on marine *Synechococcus WH7803-I*. Growth, pigmentation, and cell composition. *Deep-Sea Research*, 34, 479–495.
- Kopelevich, O., Burenkov, V., Sheberstov, S., Vazyulya, S., Kravchishina, M., Pautova, L., et al. (2013). Satellite monitoring of coccolithophore blooms in the Black Sea from ocean color data. *Remote Sensing of Environment*, <http://dx.doi.org/10.1016/j.rse.2013.09.009>.
- Krom, M. D., Emeis, K. C., & Van Cappellen, P. (2010). Why is the eastern Mediterranean phosphorus limited? *Progress in Oceanography*, 85, 236–244, <http://dx.doi.org/10.1016/j.pocean.2010.03.003>.
- Krom, M. D., Kress, N., Brenner, S., & Gordon, L. (1991). Phosphorous limitation of primary productivity in the Eastern Mediterranean Sea. *Limnology and Oceanography*, 36, 424–432.
- Lasternas, S., Agustí, D., & Duarte, C. M. (2010). Phyto- and bacterioplankton abundance and viability and their relationship with phosphorus across the Mediterranean Sea. *Aquatic Microbial Ecology*, 60, 175–191.
- Latasa, M., Estrada, M., & Delgado, M. (1992). Plankton–pigment relationships in the Northwestern Mediterranean during stratification. *Marine Ecology Progress Series*, 88, 61–73.
- Le Quéré, C., Harrison, S. P., Prentice, I. C., Buitenhuis, E. T., Aumont, O., Bopp, L., et al. (2005). Ecosystem dynamics based on plankton functional types for global ocean biogeochemistry models. *Global Change Biology*, 11, 2016–2040.
- Li, W. K. W., Subba Rao, D. V., Harrison, W. G., Smith, J. C., Cullen, J. J., & Irwin, T. (1983). Autotrophic picoplankton in the tropical ocean. *Science*, 219, 292–295.
- Loisel, H., Vantrepotte, V., Norkvist, K., Mériaux, X., Kheireddine, M., Ras, J., et al. (2011). Characterization of the bio-optical anomaly and diurnal variability of particulate matter, as seen from scattering and backscattering coefficients, in ultra-oligotrophic eddies of the Mediterranean Sea. *Biogeosciences*, 8, 3295–3317.
- Lubac, B., Loisel, H., Guiselin, N., Astoreca, R., Artigas, L. F., & Mériaux, X. (2008). Hyperspectral and multispectral ocean color inversions to detect *Phaeocystis globosa* blooms in coastal waters. *Journal of Geophysical Research*, 113, C06026, <http://dx.doi.org/10.1029/2007JC004451>.
- Mackey, M. D., Mackey, D. J., Higgins, H. W., & Wright, S. W. (1996). CHEMTAX – A program for estimating class abundances from chemical markers: Application to HPLC measurements of phytoplankton. *Marine Ecology Progress Series*, 144, 265–283.
- Marty, J. C., & Chiaverini, J. (2002). Seasonal and interannual variations in phytoplankton production at DYFAMED time-series station, northwestern Mediterranean Sea. *Deep Sea Research Part II*, 49, 2017–2030.
- Marty, J. C., & Chiaverini, J. (2010). Hydrological changes in the Ligurian Sea (NW Mediterranean, DYFAMED site) during 1995–2007 and biogeochemical consequences. *Biogeosciences*, 7, 2117–2128.
- Marty, J. C., Chiaverini, J., Pizay, M. D., & Avril, B. (2002). Seasonal and interannual dynamics of nutrients and phytoplankton pigments in the western Mediterranean Sea at the

- DYFAMED time-series station (1991–1999). *Deep Sea Research Part II: Topical Studies in Oceanography*, 49, 1965–1985.
- Masotti, I., Alvain, S., Moulin, C., & Antoine, D. (2009). *Variability in global ocean phytoplankton distribution over 1979–2007*. April. Vienna, Austria: EGU, 20–24.
- Masotti, I., Belviso, S., Alvain, S., Johnson, J. E., Bates, T. S., Tortell, P. D., et al. (2010). Spatial and temporal variability of the dimethylsulfide to chlorophyll ratio in the surface ocean: An assessment based on phytoplankton group dominance determined from space. *Biogeosciences*, 7, 3215–3237.
- Masotti, I., Moulin, C., Alvain, S., Bopp, L., Tagliabue, A., & Antoine, D. (2011). Large-scale shifts in phytoplankton groups in the Equatorial Pacific during ENSO cycles. *Biogeosciences*, 8, 539–550, <http://dx.doi.org/10.5194/bg-8-539-2011>.
- Mella-Flores, D., Mazard, S., Humily, F., Partensky, F., Mahé, F., Bariat, L., et al. (2011). Is the distribution of *Prochlorococcus* and *Synechococcus* ecotypes in the Mediterranean Sea affected by global warming? *Biogeosciences*, 8, 2785–2804.
- Mitsui, A., Kumazawa, S., Takahashi, A., Ikemoto, H., Cao, S., & Arai, T. (1986). Strategy by which unicellular cyanobacteria grow phototrophically. *Nature*, 23, 720–722.
- Moore, T. S., Dowell, M. D., & Franz, B.A. (2012). Detection of coccolithophore blooms in ocean color satellite imagery: A generalized approach for use with multiple sensors. *Remote Sensing of Environment*, 117, 249–263.
- Morel, A. (1997). Consequences of a *Synechococcus* bloom upon the optical properties of oceanic (case 1) waters. *Limnology and Oceanography*, 42, 1746–1754.
- Morel, A., & Gentili, B. (2009). The dissolved yellow substance and the shades of blue in the Mediterranean Sea. *Biogeosciences*, 6, 2625–2636, <http://dx.doi.org/10.5194/bg-6-2625-2009>.
- Moulin, C., Dulac, F., Lambert, C. E., Chazette, P., Jankowiak, I., Chatenet, B., et al. (1997). Long-term daily monitoring of Saharan dust load over ocean using Meteosat ISCCP-B2 data.2. Accuracy of the method and validation using Sun photometer measurements. *Journal of Geophysical Research – Atmospheres*, 102(D14), 16959–16969.
- Nair, A., Sathyendranath, S., Platt, T., Morales, J., Stuart, V., Forget, M. H., et al. (2008). Remote sensing of phytoplankton functional types. *Remote Sensing of Environment*, 112, 3366–3375.
- Nezlin, N.P., & DiGiacomo, P.M. (2005). Satellite ocean color observations of stormwater runoff plumes along the San Pedro Shelf (southern California) during 1997–2003. *Continental Shelf Research*, 25, 1692–1711.
- Oguz, T., Tugrul, S., Kideys, A. E., Ediger, V., & Kubilay, N. (2004). Physical and biogeochemical characteristics of the Black Sea. In A. R. Robinson, & K. H. Brink (Eds.), *The sea* (pp. 1331–1369). Cambridge (MA): Harvard University Press.
- O'Reilly, J. E., Maritorena, S., Mitchell, B. G., Siegel, D. A., Carder, K. L., Garver, S. A., et al. (1998). Ocean color chlorophyll algorithms for SeaWiFS. *Journal of Geophysical Research*, 103(C11), 24937–24953.
- O'Reilly, J. E., Maritorena, S., Siegel, D., O'Brien, M. C., Toole, D., Mitchell, B. G., Kahru, M., Chavez, F. P., Strutton, P., Cota, G., Hooker, S. B., McClain, C. R., Carder, K. L., Muller-Karger, F., Harding, L., Magnuson, A., Phinney, D., Moore, G. F., Aiken, J., Arrigo, K. R., Letelier, R., & Culver, M.9–23. (2000). Ocean color chlorophyll a algorithms for SeaWiFS, OC2, and OC4: Version 4. In S. B. Hooker, & E. R. Firestone (Eds.), *SeaWiFS postlaunch technical report series. SeaWiFS postlaunch calibration and validation analyses, part 3, Vol. 11*. (pp. 9–23). Greenbelt, Maryland: NASA Goddard Space Flight Center.
- Organelli, E., Bricaud, A., Antoine, D., & Uitz, J. (2013). Multivariate approach for the retrieval of phytoplankton size structure from measured light absorption spectra in the Mediterranean Sea (BOUSSOLE site). *Applied Optics*, 52, 2257–2273.
- Oviedo, A.M., Ziveri, P., Alvarez, M., & Tanhua, T. (2014). Is coccolithophore distribution in the Mediterranean Sea related to seawater carbonate chemistry? *Ocean Science Discussion*, 11, 613–653.
- Pael, H. W., Tucker, J., & Bland, P. (1983). Carotenoid enhancement and its role in maintaining blue-green algal (*Microcystis aeruginosa*) surface blooms. *Limnology and Oceanography*, 28, 847–857.
- Peliz, A., Marchesiello, P., Santos, A.M. P., Dubert, J., Teles-Machado, A., & Marta-Almeida, M. (2009). Surface circulation in the Gulf of Cadiz: 2. Inflow-outflow coupling and the Gulf of Cadiz slope current. *Journal of Geophysical Research*, 114, C03011, <http://dx.doi.org/10.1029/2008JC004771>.
- Peloquin, J., Swan, C., Gruber, N., Vogt, M., Claustre, H., & Ras, J. (2013). The MAREDAT global database of high performance liquid chromatography marine pigment measurements. *Earth System Science Data*, 5, 109–123.
- Platt, T., Sathyendranath, S., & Stuart, V. (2006). Why study biological oceanography? *Aquabiology*, 28, 542–557.
- Raittso, D., Lavender, S. J., Marvelias, C. D., Haralambous, J., Richardson, A. J., & Reid, P. C. (2008). Identifying four phytoplankton functional types from space: An ecological approach. *Limnology and Oceanography*, 53, 605–613.
- Ras, J., Claustre, H., Xing, X., & Uitz, J. (2011). Phytoplankton pigment distribution across the Mediterranean Sea during Spring and Autumn 2008. *SESAME Final Scientific Conference*, 4–8 April 2011, Athens.
- Ras, J., Uitz, J., & Claustre, H. (2008). Spatial variability of phytoplankton pigment distributions in the Subtropical South Pacific Ocean: Comparison between in situ and modelled data. *Biogeosciences*, 5, 353–369.
- Rudorff, N. D., & Kampel, M. (2011). Orbital remote sensing of phytoplankton functional types: A new review. *International Journal of Remote Sensing*, 33, 1967–1990.
- Sachs, J. P., & Repeta, D. J. (1999). Oligotrophy and nitrogen fixation during eastern Mediterranean sapropel events. *Science*, 286, 2485–2488.
- Santic, D., Krstulovic, N., Solic, M., & Kuspilic, G. (2011). Distribution of *Synechococcus* and *Prochlorococcus* in the central Adriatic Sea. *Acta Adriatica*, 52(1), 101–114.
- Santoleri, R., Volpe, G., Marullo, S., & Nardelli, B. B. (2008). Open waters optical remote sensing of the Mediterranean Sea. In V. Barale, & M. Gade (Eds.), *Remote sensing of the European seas* (pp. 103–116). Netherlands: Springer.
- Sathyendranath, S., Watts, L., Devred, E., Platt, T., Caverhill, C., & Maass, H. (2004). Discrimination of diatoms from other phytoplankton using ocean-colour data. *Marine Ecology Progress Series*, 272, 59–68.
- Schauer, M., Balagüe, V., Pedrós-Alio, C., & Massana, R. (2003). Seasonal changes in the taxonomic composition of bacterioplankton in a coastal oligotrophic system. *Aquatic Microbial Ecology*, 31, 163–174.
- Schoemann, V., Becquevert, S., Stefels, J., Rousseau, V., & Lancelot, C. (2005). *Phaeocystis*-like blooms in the global ocean and their controlling mechanisms: A review. *Journal of Sea Research*, 53.
- Siokou-Frangou, I., Christaki, U., Mazzocchi, M. G., Montresor, M., d'Alcalá, Ribera M., Vaqué, D., et al. (2010). Plankton in the open Mediterranean Sea: A review. *Biogeosciences*, 7, 1543–1586.
- Smyth, T. J., Moore, G. F., Groom, S. B., Land, P. E., & Tyrell, T. (2002). Optical modelling and measurements of a coccolithophore bloom. *Applied Optics*, 41, 7679–7688.
- Socal, G., Boldrin, A., Bianchi, F., Civitarese, G., De Lazzari, A., Rabitti, S., et al. (1999). Nutrient, particulate matter and phytoplankton variability in the photic layer of the Otranto Strait. *Journal of Marine Systems*, 20, 381–398.
- Sommaruga, R., Hofer, J. S., Alonso-Saez, L., & Gasol, J. M. (2005). Differential sunlight sensitivity of picophytoplankton from surface Mediterranean coastal waters. *Applied and Environmental Microbiology*, 71, 2154–2157.
- Subramaniam, A., Brown, C. W., Hood, R. R., Carpenter, E. J., & Capone, D. G. (2001). Detecting *Trichodesmium* blooms in SeaWiFS imagery. *Deep Sea Research Part II: Topical Studies in Oceanography*, 49, 107–121.
- Subramaniam, A., Carpenter, E. J., & Falkowski, P. G. (1999). Optical properties of the marine diazotrophic cyanobacteria *Trichodesmium* spp.: II. A reflectance model for remote-sensing. *Limnology and Oceanography*, 44, 618–627.
- Tanhua, T., Hainbucher, D., Schröder, K., Cardin, V., Álvarez, M., & Civitarese, G. (2013). The Mediterranean Sea system: A review and an introduction to the special issue. *Ocean Science Discussion*, 10, 581–617.
- The MerMex Group (2011). Marine ecosystems' responses to climatic and anthropogenic forcings in the Mediterranean. *Progress in Oceanography*, 91, 97–166, <http://dx.doi.org/10.1016/j.pocean.2011.02.003>.
- Trees, C. C., Clark, D. K., Bidigare, R. R., Ondrusek, M. E., & Mueller, J. L. (2000). Accessory pigments versus chlorophyll-a concentrations within the euphotic zone: A ubiquitous relationship. *Limnology and Oceanography*, 45, 1130–1143.
- Tyrell, T., Holligan, P. M., & Mobley, C. D. (1999). Optical impacts of oceanic coccolithophore blooms. *Journal of Geophysical Research*, 104, 3223–3241.
- Uitz, J., Claustre, H., Morel, A., & Hooker, S. B. (2006). Vertical distribution of phytoplankton communities in Open Ocean: An assessment based on surface chlorophyll. *Journal of Geophysical Research*, 111 CO8005.
- Uitz, J., Stramski, D., Gentili, B., D'Ortenzio, F., & Claustre, H. (2012). Estimates of phytoplankton class-specific and total primary production in the Mediterranean Sea from satellite ocean color observations. *Global Biogeochemical Cycles*, 26 GB2024.
- Vaulot, D., Partensky, F., Neveux, J., Mantoura, F. C., & Llewellyn, C. A. (1990). Winter presence of prochlorophytes in surface waters of the northwestern Mediterranean Sea. *Limnology and Oceanography*, 35, 1156–1164.
- Vidussi, F., Claustre, H., Manca, B., Luchetta, A., & Marty, J. C. (2001). Phytoplankton pigment distribution in relation to the upper thermocline circulation in the Eastern Mediterranean Sea during winter. *Journal of Geophysical Research*, 106, 19939–19956.
- Vidussi, F., Marty, J. C., & Chiavérini, J. (2000). Phytoplankton pigment variations during the transition from spring bloom to oligotrophy in the northwestern Mediterranean Sea. *Deep-Sea Research*, 47, 423–445.
- Volpe, G., Santoleri, R., Vellucci, V., d'Alcalà, Ribera M., Marullo, S., & D'Ortenzio, F. (2007). The colour of the Mediterranean Sea: Global versus regional bio-optical algorithms evaluation and implication for satellite chlorophyll estimates. *Remote Sensing of Environment*, 107, 625–638.
- Wright, S. W., & Jeffrey, S. W. (1987). Fucoxanthin pigment markers of marine phytoplankton analysed by HPLC and HPTLC. *Marine Ecology Progress Series*, 38, 259–266.
- Zingone, A., Chrétiennot-Dinet, M. J., Lange, M., & Medlin, L. (1999). Morphological and genetic characterization of *Phaeocystis cordata* and *P. jahnnii* (Prymnesiophyceae), two new species from the Mediterranean Sea. *Journal of Phycology*, 35, 1322–1337.